Available online at www.sciencedirect.com
SCIENCE DIRECT®
Journal of Computational Physics 202 (2005) 602–644
JOURNAL OF COMPUTATIONAL PHYSICS
www.elsevier.com/locate/jcp

Numerical approximation of the Vlasov–Poisson–Fokker–Planck system in one dimension

Stephen Wollman *, Ercument Ozizmir

The College of Staten Island, CUNY, 2800 Victory Boulevard, Staten Island, NY 10314, USA

Received 21 October 2003; received in revised form 1 July 2004; accepted 28 July 2004
Available online 16 September 2004

Abstract

A numerical method is developed for approximating the Vlasov–Poisson–Fokker–Planck system in one dimension. This system of equations is a mathematical model for an electrostatic plasma in which collisions between the electron distribution and a surrounding medium are taken into account. The numerical procedure combines a deterministic particle type computation with a process for periodically reconstructing the distribution function on a fixed grid. The method is tested on some computational examples and shown to be stable and accurate on an extended interval of time. Some comparisons are also made with other methods of approximation for the Vlasov–Poisson–Fokker–Planck system.

MSC: 65M06; 65M25; 82D10
Keywords: Collisional plasma; Vlasov–Poisson–Fokker–Planck system; Particle method

1. The system of equations

The Vlasov–Poisson–Fokker–Planck system in one dimension with periodic boundary conditions is given as follows: for the region of phase space $A = \{(x,v)/0 \leqslant x \leqslant L,\ -\infty < v < -\infty\}$ and $t \in [0,T]$ then $f(x,v,t)$ is the phase space distribution function defined on $A \times [0,T]$ which satisfies the system of equations

$$\frac{\partial f}{\partial t} + v\frac{\partial f}{\partial x} + (E(x,t) - \beta v)\frac{\partial f}{\partial v} - \beta f - q\frac{\partial^2 f}{\partial v^2} = 0, \tag{1.1}$$

$$f(x,v,0) = f_0(x,v),$$

* Corresponding author. Tel.: +1 718 982 3614.
E-mail addresses: wollman@math.csi.cuny.edu (S. Wollman), ozizmir@postbox.csi.cuny.edu (E. Ozizmir).

0021-9991/$ - see front matter
doi:10.1016/j.jcp.2004.07.017

where

$$E(x,t) = \frac{\partial \phi}{\partial x}$$

and $\phi(x,t)$ is the solution to

$$\frac{\partial^2 \phi}{\partial x^2} = \rho(x,t), \tag{1.2}$$

$$\phi(0,t) = \phi(L,t) = 0,$$

with

$$\rho(x,t) = \int_{-\infty}^{\infty} f(x,v,t)\mathrm{d}v - h(x). \tag{1.3}$$

The function $h(x)$ represents a fixed background charge. In addition it is assumed that

$$f_0(0,v) = f_0(L,v)$$

and

$$\int_0^L \int_{-\infty}^{\infty} f_0(x,v)\mathrm{d}v\,\mathrm{d}x = \int_0^L h(x)\mathrm{d}x, \tag{1.4}$$

the latter being a condition for total charge neutrality. This system of equations describes the time evolution of an electrostatic plasma. In this plasma model collisions between the elements of the electron distribution, $f(x,v,t)$, and a surrounding medium are taken into account through the inclusion of the terms involving q and β.

We can assume the existence and uniqueness of a solution to (1.1) and (1.2) of class $C^2(A \times [0,T])$ and which can be extended periodically to each strip $nL \leqslant x \leqslant (n+1)L$, $-\infty < v < \infty$, $0 \leqslant t \leqslant T$. A proof of global existence and uniqueness of the solution to the Vlasov–Poisson–Fokker–Planck system in one dimension is contained in [17]. If $f_0(x,v) \geqslant 0$ then it can be shown that $f(x,v,t) \geqslant 0$ for $t > 0$ and if

$$\int_0^L \int_{-\infty}^{\infty} f_0(x,v)\mathrm{d}v\,\mathrm{d}x$$

is finite then

$$\int_0^L \int_{-\infty}^{\infty} f(x,v,t)\mathrm{d}v\,\mathrm{d}x = \int_0^L \int_{-\infty}^{\infty} f_0(x,v)\mathrm{d}v\,\mathrm{d}x. \tag{1.5}$$

Given (1.4) then

$$\int_0^L \rho(x,t)\mathrm{d}x = 0, \quad t \geqslant 0.$$

Also, the boundary condition for ϕ implies that

$$\int_0^L E(x,t)\mathrm{d}x = 0, \quad t \geqslant 0.$$

In terms of the Green's function for the boundary value problem (1.2) then

$$E(x,t) = \int_0^L K(x,\bar{x})\rho(\bar{x},t)\mathrm{d}\bar{x}$$

and

$$K(x,\bar{x}) = \begin{cases} \bar{x}/L, & 0 < \bar{x} \leqslant x, \\ \frac{\bar{x}}{L} - 1, & x < \bar{x} \leqslant L. \end{cases}$$

Thus

$$E(x,t) = \int_0^L K(x,\bar{x}) \left(\int_{-\infty}^{\infty} f \, \mathrm{d}v - h(\bar{x}) \right) \mathrm{d}\bar{x} = \int_0^L \int_{-\infty}^{\infty} K(x,\bar{x}) f(\bar{x},v,t) \mathrm{d}v \, \mathrm{d}\bar{x} - \int_0^L K(x,\bar{x}) h(\bar{x}) \mathrm{d}\bar{x}. \tag{1.6}$$

One way of numerically approximating solutions to (1.1) and (1.2) is the random particle method. An analysis of the method is in [9], and a computational study of this method is carried out in [1]. Some computational work on the random particle method is also done in [15]. Papers have also been written on deterministic methods for numerically solving the system [10,13–15]. The approach taken in these papers is to approximate the solution to (1.1) and (1.2) by computing the solution along characteristic curves associated with the first order transport part of (1.1). In the present paper, we consider another way of doing this. A type of deterministic particle method is formulated based on characteristic trajectories. However, over a relatively long time interval the particle method alone develops numerical instabilities. Thus, limits are set on the length of time for which the particle computation is applied, and at the end of this time interval the approximate distribution function is reconstructed on a fixed grid. With the reconstructed solution serving as a new set of initial data the particle method is restarted and continued for another time interval. Combining the particle type computation along characteristic trajectories with the periodic regriding of the distribution function leads to a numerical method that is stable and accurate on an extended interval of time. Aspects of this paper were presented in preliminary form in [20].

To put this system into a different form for approximation we start with a somewhat simpler linear initial value problem in all of phase space in which $E(x,t)$ is a known function.

$$\frac{\partial f}{\partial t} + v\frac{\partial f}{\partial x} + (E(x,t) - \beta v)\frac{\partial f}{\partial v} - \beta f - q\frac{\partial^2 f}{\partial v^2} = 0, \tag{1.7}$$

$$f(x,v,0) = f_0(x,v), \quad -\infty < x < \infty, \ -\infty < v < \infty.$$

The characteristic system associated with the equation

$$\frac{\partial f}{\partial t} + v\frac{\partial f}{\partial x} + (E(x,t) - \beta v)\frac{\partial f}{\partial v} = 0 \tag{1.8}$$

is

$$\frac{\mathrm{d}x}{\mathrm{d}t} = v, \quad x(0) = x_0, \tag{1.9}$$

$$\frac{\mathrm{d}v}{\mathrm{d}t} = E(x(t),t) - \beta v, \quad v(0) = v_0. \tag{1.10}$$

The solution to (1.9) and (1.10) is

$$x(t) = x(x_0,v_0,t), \quad v(t) = v(x_0,v_0,t),$$

continuously differentiate functions of x_0, v_0 and t. For each t the transformation of R_2 given by

$$(x_0,v_0) \ \rightarrow \ (x(x_0,v_0,t), v(x_0,v_0,t)) \tag{1.11}$$

has nonzero Jacobian and is therefore invertible. Let the functions

$$x_0 = x_0(x,v,t), \quad v_0 = v_0(x,v,t) \tag{1.12}$$

define the inverse transformation $(x,v) \to (x_0(x,v,t), v_0(x,v,t))$. Following an approach taken by Chandrasekhar in [5], Eq. (1.7) is written in terms of the variables x_0, v_0 and t with x_0, v_0 given by the functions (1.12). Using the fact that the functions (1.12) are independent integrals of (1.9) and (1.10), in terms of x_0, v_0, t, Eq. (1.7) is

$$\frac{\partial f}{\partial t} - \beta f - q\left[\left(\frac{\partial x_0}{\partial v}\right)^2 \frac{\partial^2 f}{\partial x_0^2} + 2\left(\frac{\partial x_0}{\partial v}\right)\left(\frac{\partial v_0}{\partial v}\right)\frac{\partial^2 f}{\partial x_0\,\partial v_0} + \left(\frac{\partial v_0}{\partial v}\right)^2 \frac{\partial^2 f}{\partial v_0^2} + \frac{\partial^2 x_0}{\partial v^2}\frac{\partial f}{\partial x_0} + \frac{\partial^2 v_0}{\partial v^2}\frac{\partial f}{\partial v_0}\right] = 0. \tag{1.13}$$

If $f(x_0,v_0,t)$ is the solution to (1.13) then let

$$f(x_0, v_0, t) = \mathrm{e}^{\beta t} g(x_0, v_0, t).$$

Then

$$\frac{\partial f}{\partial t} = \mathrm{e}^{\beta t}\frac{\partial g}{\partial t} + \beta\,\mathrm{e}^{\beta t} g$$

and substituting into (1.13) the equation for $g(x_0,v_0,t)$ is

$$\frac{\partial g}{\partial t} - q\left[\left(\frac{\partial x_0}{\partial v}\right)^2 \frac{\partial^2 g}{\partial x_0^2} + 2\left(\frac{\partial x_0}{\partial v}\right)\left(\frac{\partial v_0}{\partial v}\right)\frac{\partial^2 g}{\partial x_0\,\partial v_0} + \left(\frac{\partial v_0}{\partial v}\right)^2 \frac{\partial^2 g}{\partial v_0^2} + \frac{\partial^2 x_0}{\partial v^2}\frac{\partial g}{\partial x_0} + \frac{\partial^2 v_0}{\partial v^2}\frac{\partial g}{\partial v_0}\right] = 0. \tag{1.14}$$

We want to write (1.14) with coefficients in terms of x_0, v_0, t. The Jacobian of the transformation (1.11) is $\frac{\partial(x,v)}{\partial(x_0,v_0)} = |Q|$ where

$$Q = \begin{pmatrix} \frac{\partial x}{\partial x_0} & \frac{\partial x}{\partial v_0} \\ \frac{\partial v}{\partial x_0} & \frac{\partial v}{\partial v_0} \end{pmatrix}.$$

Following the methods of [8] we determine that

$$\frac{\partial x_0}{\partial v} = -\frac{1}{|Q|}\frac{\partial x}{\partial v_0}, \quad \frac{\partial v_0}{\partial v} = \frac{1}{|Q|}\frac{\partial x}{\partial x_0},$$

$$\frac{\partial^2 x_0}{\partial v^2} = \frac{1}{|Q|^3}\left(\frac{\partial v}{\partial v_0}P_1 - \frac{\partial x}{\partial v_0}P_2\right), \quad \frac{\partial^2 v_0}{\partial v^2} = \frac{1}{|Q|^3}\left(\frac{\partial x}{\partial x_0}P_2 - \frac{\partial v}{\partial x_0}P_1\right),$$

where

$$P_1 = -\frac{\partial^2 x}{\partial x_0^2}\left(\frac{\partial x}{\partial v_0}\right)^2 + 2\frac{\partial^2 x}{\partial x_0\,\partial v_0}\left(\frac{\partial x}{\partial v_0}\right)\left(\frac{\partial x}{\partial x_0}\right) - \frac{\partial^2 x}{\partial v_0^2}\left(\frac{\partial x}{\partial x_0}\right)^2, \tag{1.15}$$

$$P_2 = -\frac{\partial^2 v}{\partial x_0^2}\left(\frac{\partial x}{\partial v_0}\right)^2 + 2\frac{\partial^2 v}{\partial x_0\,\partial v_0}\left(\frac{\partial x}{\partial v_0}\right)\left(\frac{\partial x}{\partial x_0}\right) - \frac{\partial^2 v}{\partial v_0^2}\left(\frac{\partial x}{\partial x_0}\right)^2. \tag{1.16}$$

We compute the determinant of Q

$$|Q| = |Q^{\mathrm{T}}| = \begin{vmatrix} \frac{\partial x}{\partial x_0} & \frac{\partial v}{\partial x_0} \\ \frac{\partial x}{\partial v_0} & \frac{\partial v}{\partial v_0} \end{vmatrix},$$

$$\begin{aligned} \frac{\mathrm{d}|Q|}{\mathrm{d}t} &= \begin{vmatrix} \frac{\mathrm{d}}{\mathrm{d}t}\left(\frac{\partial x}{\partial x_0}\right) & \frac{\partial v}{\partial x_0} \\ \frac{\mathrm{d}}{\mathrm{d}t}\left(\frac{\partial x}{\partial v_0}\right) & \frac{\partial v}{\partial v_0} \end{vmatrix} + \begin{vmatrix} \frac{\partial x}{\partial x_0} & \frac{\mathrm{d}}{\mathrm{d}t}\left(\frac{\partial v}{\partial x_0}\right) \\ \frac{\partial x}{\partial v_0} & \frac{\mathrm{d}}{\mathrm{d}t}\left(\frac{\partial v}{\partial v_0}\right) \end{vmatrix} \\ &= \begin{vmatrix} \frac{\partial v}{\partial x_0} & \frac{\partial v}{\partial x_0} \\ \frac{\partial v}{\partial v_0} & \frac{\partial v}{\partial v_0} \end{vmatrix} + \begin{vmatrix} \frac{\partial x}{\partial x_0} & \frac{\partial E}{\partial x}\frac{\partial x}{\partial x_0} - \beta\frac{\partial v}{\partial x_0} \\ \frac{\partial x}{\partial v_0} & \frac{\partial E}{\partial x}\frac{\partial x}{\partial v_0} - \beta\frac{\partial v}{\partial v_0} \end{vmatrix} \\ &= -\beta\begin{vmatrix} \frac{\partial x}{\partial x_0} & \frac{\partial v}{\partial x_0} \\ \frac{\partial x}{\partial v_0} & \frac{\partial v}{\partial v_0} \end{vmatrix} = -\beta|Q|. \end{aligned}$$

Also

$$|Q|(0) = \begin{vmatrix} \frac{\partial x_0}{\partial x_0} & \frac{\partial v_0}{\partial x_0} \\ \frac{\partial x_0}{\partial v_0} & \frac{\partial v_0}{\partial v_0} \end{vmatrix} = \begin{vmatrix} 1 & 0 \\ 0 & 1 \end{vmatrix} = 1.$$

Thus

$$\frac{\mathrm{d}|Q|}{\mathrm{d}t} = -\beta|Q|, \quad |Q|(0) = 1,$$

so

$$|Q| = \mathrm{e}^{-\beta t}. \tag{1.17}$$

Eq. (1.14) is therefore written as

$$\frac{\partial g}{\partial t} = q\left[(a(x_0,v_0,t))^2\frac{\partial^2 g}{\partial x_0^2} - 2a(x_0,v_0,t)b(x_0,v_0,t)\frac{\partial^2 g}{\partial x_0\,\partial v_0} + (b(x_0,v_0,t))^2\frac{\partial^2 g}{\partial v_0^2} + c(x_0,v_0,t)\frac{\partial g}{\partial x_0} + d(x_0,v_0,t)\frac{\partial g}{\partial v_0}\right], \tag{1.18}$$

$$g(x_0,v_0,0) = f_0(x_0,v_0),$$

$$a(x_0,v_0,t) = \mathrm{e}^{\beta t}\frac{\partial x}{\partial v_0}(x_0,v_0,t), \quad b(x_0,v_0,t) = \mathrm{e}^{\beta t}\frac{\partial x}{\partial x_0}(x_0,v_0,t),$$

$$c(x_0,v_0,t) = \mathrm{e}^{3\beta t}\left(\frac{\partial v}{\partial v_0}P_1 - \frac{\partial x}{\partial v_0}P_2\right), \quad d(x_0,v_0,t) = \mathrm{e}^{3\beta t}\left(\frac{\partial x}{\partial x_0}P_2 - \frac{\partial v}{\partial x_0}P_1\right),$$

where P_1, P_2 are given by (1.15) and (1.16) and $x(x_0,v_0,t)$, $v(x_0,v_0,t)$ is the solution to (1.9) and (1.10). In terms of the solution to (1.18) and the inverse functions (1.12) the solution to (1.7) is written

$$f(x,v,t) = \mathrm{e}^{\beta t}g(x_0(x,v,t),v_0(x,v,t),t). \tag{1.19}$$

For the periodic problem (1.1) and (1.2) some modifications are made in the formulation given so far. In (1.18) it is now assumed that $0 \leqslant x_0 \leqslant L$, and we include the boundary condition $g(0,v_0,t) = g(L,v_0,t)$. The boundary condition in v_0 is $\lim_{|v_0|\to\infty} g(x_0,v_0,t) = 0$. The first order equation (1.8) is defined for $A = \{(x,v)/ 0 \leqslant x \leqslant L, -\infty < v < \infty\}$. The transformation (1.11) and the inverse (1.12) are regarded as transformations of A onto A.

Referring now to the nonlinear problem (1.1) and (1.2) the field $E(x,t)$ is given by (1.6). By a change of variable in the integral based on (1.11) and noting that $f(x,v,t)$ has an expression of the form (1.19)

$$\begin{aligned}\int_0^L\int_{-\infty}^{\infty} K(x,\bar{x})f(\bar{x},v,t)\mathrm{d}v\,\mathrm{d}x &= \int_0^L\int_{-\infty}^{\infty} K(x,\bar{x}(y_0,w_0,t))\mathrm{e}^{\beta t}g(y_0,w_0,t)\left|\frac{\partial(\bar{x},v)}{\partial(y_0,w_0)}\right|\mathrm{d}y_0\,\mathrm{d}w_0 \\ &= \int_0^L\int_{-\infty}^{\infty} K(x,\bar{x}(y_0,w_0,t))\mathrm{e}^{\beta t}g(y_0,w_0,t)\mathrm{e}^{-\beta t}\,\mathrm{d}w_0\,\mathrm{d}y_0 \\ &= \int_0^L\int_{-\infty}^{\infty} K(x,\bar{x}(y_0,w_0,t))g(y_0,w_0,t)\mathrm{d}w_0\,\mathrm{d}y_0.\end{aligned}$$

Thus in terms of the solution to (1.18) with periodic boundary conditions the field $E(x,t)$ is expressed as

$$E(x,t) = \int_0^L\int_{-\infty}^{\infty} K(x,\bar{x}(y_0,w_0,t))g(y_0,w_0,t)\mathrm{d}w_0\,\mathrm{d}y_0 - \int_0^L K(x,\bar{x})h(\bar{x})\mathrm{d}\bar{x}. \tag{1.20}$$

In order to more efficiently solve (1.18) for $-\infty < v_0 < \infty$ we make a further transformation of independent variable [4, p. 708]. Let

$$v_0 = \frac{cu}{\sqrt{1-u^2}}, \quad -1 < u < 1, \ -\infty < v_0 < \infty,$$

$$\frac{\partial g}{\partial v_0} = \frac{1}{c}(1-u^2)^{3/2}\frac{\partial g}{\partial u},$$

$$\frac{\partial^2 g}{\partial v_0^2} = 1/c^2(1-u^2)^3\frac{\partial^2 g}{\partial u^2} - 3/c^2(1-u^2)^2 u\frac{\partial g}{\partial u} = \frac{(1-u^2)^{3/2}}{c}\frac{\partial}{\partial u}\left(\frac{(1-u^2)^{3/2}}{c}\frac{\partial g}{\partial u}\right).$$

Under this transformation the boundary condition of (1.18) for $|v_0| \to \infty$ becomes $g = 0$ at $u = \pm 1$.

In terms of the variables x_0, u, t, $0 \leqslant x_0 \leqslant L$, $-1 < u < 1$, $v_0(u) = cu/\sqrt{1-u^2}$, we solve the set of equations

$$\frac{\partial g}{\partial t} = q\left[(a(x_0, v_0(u), t))^2\frac{\partial^2 g}{\partial x_0^2} - 2a(x_0, v_0(u), t)b(x_0, v_0(u), t)\frac{(1-u^2)^{3/2}}{c}\frac{\partial^2 g}{\partial x_0\,\partial u}\right.$$
$$\left. + (b(x_0, v_0(u), t))^2\frac{(1-u^2)^{3/2}}{c}\frac{\partial}{\partial u}\frac{(1-u^2)^{3/2}}{c}\frac{\partial g}{\partial u} + c(x_0, v_0(u), t)\frac{\partial g}{\partial x_0} + d(x_0, v_0(u), t)\frac{(1-u^2)^{3/2}}{c}\frac{\partial g}{\partial u}\right], \tag{1.21}$$

$$g(x_0, u, 0) = f_0\left(x_0, \frac{cu}{\sqrt{1-u^2}}\right), \quad g(0, u, t) = g(L, u, t), \quad g(x_0, -1, t) = g(x_0, 1, t) = 0,$$

$$a(x_0, v_0(u), t) = \mathrm{e}^{\beta t}\frac{\partial x}{\partial v_0}, \quad b(x_0, v_0(u), t) = \mathrm{e}^{\beta t}\frac{\partial x}{\partial x_0}, \tag{1.22}$$

$$c(x_0, v_0, t) = \mathrm{e}^{3\beta t}\left(\frac{\partial v}{\partial v_0}P_1 - \frac{\partial x}{\partial v_0}P_2\right), \quad d(x_0, v_0, t) = \mathrm{e}^{3\beta t}\left(\frac{\partial x}{\partial x_0}P_2 - \frac{\partial v}{\partial x_0}P_1\right), \tag{1.23}$$

where $x(x_0,v_0(u),t)$, $v(x_0,v_0(u),t)$ are the solutions to

$$\frac{\mathrm{d}x}{\mathrm{d}t} = v, \quad x(0) = x_0, \tag{1.24}$$

$$\frac{\mathrm{d}v}{\mathrm{d}t} = E(x(x_0, v_0(u), t), t) - \beta v, \tag{1.25}$$

$$v(0) = v_0(u) = \frac{cu}{\sqrt{1-u^2}}$$

and where P_1, P_2 are given by (1.15) and (1.16) now regarded as functions of x_0, u, t.

The integral for the electric field given by (1.20) is transformed as

$$\int_0^L\int_{-\infty}^{\infty} K(x(x_0, v_0, t), x(y_0, w_0, t))g(y_0, w_0, t)\mathrm{d}w_0\,\mathrm{d}y_0$$
$$= \int_0^L\int_{-1}^{1} K(x(x_0, v_0(u), t), x(y_0, w_0(\bar{u}), t))g(y_0, \bar{u}, t)\left|\frac{\partial(y_0, w_0)}{\partial(y_0, \bar{u})}\right|\mathrm{d}\bar{u}\,\mathrm{d}y_0$$
$$= \int_0^L\int_{-1}^{1} K(x(x_0, v_0(u), t), x(y_0, w_0(\bar{u}), t))g(y_0, \bar{u}, t)\frac{c}{(1-\bar{u}^2)^{3/2}}\,\mathrm{d}\bar{u}\,\mathrm{d}y_0,$$

since the Jacobian for the change of variable (y_0,w_0) to $(y_0, \bar{u})$ is

$$\frac{\partial(y_0, w_0)}{\partial(y_0, \bar{u})} = \frac{c}{(1-\bar{u}^2)^{3/2}}. \tag{1.26}$$

Thus in terms of the solution to (1.21) the function $E(x,t)$ in (1.25) is written

$$E(x(x_0, v_0(u), t), t) = \int_0^L \int_{-1}^1 K(x(x_0, v_0(u), t), x(y_0, w_0(\bar{u}), t)) g(y_0, \bar{u}, t) \frac{c}{(1-\bar{u}^2)^{3/2}} \, \mathrm{d}\bar{u} \, \mathrm{d}y_0 - \int_0^L K(x(x_0, v_0(u), t), \bar{x}) h(\bar{x}) \mathrm{d}\bar{x}.$$

If $v_0 = \frac{cu}{\sqrt{1-u^2}}$ then $u = u(v_0) = \frac{v_0}{\sqrt{v_0^2+c^2}}$. The solution to (1.1) is written in terms of the solution to (1.21) and the inverse transformation (1.12) as

$$f(x, v, t) = \mathrm{e}^{\beta t} g(x_0(x, v, t), u(v_0(x, v, t)), t). \tag{1.27}$$

The functions $a(x_0,v_0(u),t)$, $b(x_0,v_0(u),t)$ can be obtained by differentiating (1.24) and (1.25) and solving the equations

$$\frac{\mathrm{d}}{\mathrm{d}t}\left(\frac{\partial x}{\partial v_0}\right) = \frac{\partial v}{\partial v_0}, \quad \frac{\partial x}{\partial v_0}(0) = 0, \tag{1.28}$$

$$\frac{\mathrm{d}}{\mathrm{d}t}\left(\frac{\partial v}{\partial v_0}\right) = \frac{\partial E}{\partial x}(x(x_0, v_0(u), t), t)\left(\frac{\partial x}{\partial v_0}\right) - \beta\left(\frac{\partial v}{\partial v_0}\right), \quad \frac{\partial v}{\partial v_0}(0) = 1 \tag{1.29}$$

and

$$\frac{\mathrm{d}}{\mathrm{d}t}\left(\frac{\partial x}{\partial x_0}\right) = \frac{\partial v}{\partial x_0}, \quad \frac{\partial x}{\partial x_0}(0) = 1, \tag{1.30}$$

$$\frac{\mathrm{d}}{\mathrm{d}t}\left(\frac{\partial v}{\partial x_0}\right) = \frac{\partial E}{\partial x}(x(x_0, v_0(u), t), t)\left(\frac{\partial x}{\partial x_0}\right) - \beta\left(\frac{\partial v}{\partial x_0}\right), \quad \frac{\partial v}{\partial x_0}(0) = 0. \tag{1.31}$$

Then $a(x_0,v_0(u),t)$, $b(x_0,v_0(u),t)$ are given by (1.22). By (1.2) $\frac{\partial E}{\partial x}(x(x_0, v_0(u), t), t) = \rho(x(x_0, v_0(u), t), t)$.

For the coefficients $c(x_0,v_0(u),t)$, $d(x_0,v_0(u),t)$ it is, in addition, necessary to solve equations for the second partial derivatives

$$\frac{\mathrm{d}}{\mathrm{d}t}\left(\frac{\partial^2 x}{\partial x_0^s \, \partial v_0^r}\right) = \frac{\partial^2 v}{\partial x_0^s \, \partial v_0^r}, \quad \frac{\partial^2 x}{\partial x_0^s \, \partial v_0^r}(0) = 0, \tag{1.32}$$

$$\frac{\mathrm{d}}{\mathrm{d}t}\left(\frac{\partial^2 v}{\partial x_0^s \, \partial v_0^r}\right) = \frac{\partial E}{\partial x}\left(\frac{\partial^2 x}{\partial x_0^s \, \partial v_0^r}\right) - \beta\left(\frac{\partial^2 v}{\partial x_0^s \, \partial v_0^r}\right) + \frac{\partial^2 E}{\partial x^2}\left(\frac{\partial x}{\partial x_0}\right)^s \left(\frac{\partial x}{\partial v_0}\right)^r, \quad \frac{\partial^2 v}{\partial x_0^s \, \partial v_0^r}(0) = 0, \tag{1.33}$$

$$s, r = 0, 1, 2, \quad s + r = 2.$$

Then $c(x_0,v_0(u),t)$, $d(x_0,v_0(u),t)$ are given by (1.23).

The solution to (1.1) and (1.2) can be given in terms of a sequence of solutions to (1.21). We proceed as follows: for the time interval $[0,T]$ let T_1 be such that $T/T_1 = M$ an integer. The interval $[0,T]$ is divided into subintervals $[lT_1,(l+1)T_1]$, $l = 0, 1, \ldots, M-1$. The relationship between $g(x_0,u,t)$ as a solution to (1.21) and $f(x,v,t)$ as a solution to (1.1) is given by (1.27). We let the time variable be $\bar{t}$ so that $f(x, v, \bar{t})$ is the solution to (1.1) with initial function $f_0(x,v)$ and $\bar{t} \in [0, T]$. On the time interval $lT_1 \leqslant \bar{t} \leqslant (l+1)T_1$ let $t = \bar{t} - lT_1$. Then

$$f(x, v, \bar{t}) = \mathrm{e}^{\beta t} g(x_0(x, v, t), u(v_0(x, v, t)), t), \quad t \in [0, T_1] \tag{1.34}$$

in which $g(x_0,u,t)$ is the solution to (1.21), combined with (1.24), (1.25), (1.28)–(1.33), such that $g(x_0,u,0) = f\left(x_0, \frac{cu}{\sqrt{1-u^2}}, lT_1\right)$. If $l = 0$ then $f(x,v,lT_1) = f_0(x,v)$. If $l > 0$ then $f(x,v,lT_1) = e^{\beta T_1} g(x_0(x,v,T_1), u(v_0(x,v,T_1)), T_1)$ such that $g(x_0,u,t)$ is the solution to (1.21) for $t \in [0,T_1]$ with initial data $g(x_0,u,0) = f\left(x_0, \frac{cu}{\sqrt{1-u^2}}, (l-1)T_1\right)$. The numerical method is a discretization of this procedure.

2. The discrete approximation

A method is outlined for approximating the solution to (1.1) and (1.2).

2.1. Partition of phase space and time intervals

Several domains of definition for functions have been defined. Phase space is the (x,v) domain given by

$$A = \{(x,v)/0 \leqslant x \leqslant L,\ -\infty < v < \infty\}.$$

The (x_0,v_0) domain is

$$A_0 = \{(x_0,v_0)/0 \leqslant x_0 \leqslant L,\ -\infty < v_0 < \infty\},$$

such that $x_0 = x_0(x,v,t)$, $v_0 = v_0(x,v,t)$ and $(x_0(x,v,t), v_0(x,v,t))$ the functions defined by (1.12). The (x_0,u) domain is

$$\Omega = \{(x_0,u)/0 \leqslant x_0 \leqslant L,\ -1 < u < 1\},$$

such that $v_0 = cu/\sqrt{1-u^2}$.

The domain Ω is partitioned as follows: given integers N_x, N_v let $\Delta x_0 = L/N_x$, $\Delta u = 2/(N_v+1)$. Then

$$\begin{aligned} x_{0_i} &= \left(i - \frac{1}{2}\right)\Delta x_0, \quad i = 1,\ldots,N_x, \\ u_j &= -1 + j\Delta u, \quad j = 1,\ldots,N_v. \end{aligned} \tag{2.1}$$

Thus the region

$$\left\{(x_0,u)/0 \leqslant x_0 \leqslant L, \quad -\frac{N_v}{N_v+1} \leqslant u \leqslant \frac{N_v}{N_v+1}\right\} \subset \Omega$$

is subdivided into a uniform rectangular grid with (x_{0_i}, u_j) the center of the i,j rectangle on the grid. The region

$$\left\{(x_0,u)/0 \leqslant x_0 \leqslant L, \quad -1 < u < -\frac{N_v}{N_v+1} \quad \text{or} \quad \frac{N_v}{N_v+1} < u < 1\right\}$$

is the part of Ω associated with points at infinity at which the distribution function is zero.

Let

$$v_{0_j} = \frac{cu_j}{\sqrt{1-u_j^2}}. \tag{2.2}$$

The point (x_{0_i}, u_j) in Ω corresponds to the point (x_{0_i}, v_{0_j}) in A_0.

Given the time interval $[0,T]$ let $T_1 < T$ be such that $MT_1 = T$ for the positive integer M. For positive integer N_g let $\Delta t = T_1/N_g$. Then $t_n = n\Delta t$, $n = 0, 1, \ldots, N_g$ is a partition of the time interval $[0,T_1]$. Let $\tau_l = lT_1 = 0$, $l = 0, 1, \ldots, M$ and $\bar{t}_k = \tau_l + t_n$ for $k = lN_g + n$. Eqs. (1.21), (1.24), (1.25), (1.28)–(1.33) are discretized on the time interval $[0,T_1]$ with discrete time parameter, Δt. The approximate distribution function is reconstructed on a fixed grid at times τ_l, $l = 0, 1, \ldots, M$. The actual time of the discrete approximation to (1.1) and (1.2) is given by $\bar{t}_k, k = 0, 1, \ldots, N_t$ where $N_t = MN_g$.

2.2. The deterministic particle method on the time interval $[0,T_1]$

2.2.1. The initial data

On the time interval $[lT_1,(l+1)T_1]$, $l=0,1,\ldots,M-1$ the solution to (1.1) and (1.2) is obtained by approximating the solution to (1.21), (1.24), (1.25), (1.28)–(1.33) in which the initial function for (1.21) is $f\left(x_0,\frac{cu}{\sqrt{1-u^2}},lT_1\right)$ with $f(x,v,t)$ the solution to (1.1). If $l=0$ then $f\left(x_0,\frac{cu}{\sqrt{1-u^2}},lT_1\right)=f_0\left(x_0,\frac{cu}{\sqrt{1-u^2}}\right)$. The initial function $f_0(x,v)$ for (1.1) satisfies Eq. (1.4). In terms of the variables x_0, u and given (1.26) then when $l=0$ the initial data for (1.21) satisfies

$$\int_0^L\int_{-1}^1 g(x_0,u,0)\frac{c}{(1-u^2)^{3/2}}\,du\,dx_0=\int_0^L\int_{-1}^1 f_0\left(x_0,\frac{cu}{\sqrt{1-u^2}}\right)\frac{c}{(1-u^2)^{3/2}}\,du\,dx_0=\int_0^L h(x_0)dx_0.$$

Let

$$\bar{g}^0_{i,j}=f_0(x_{0_i},v_{0_j}),\quad v_{0_j}=\frac{cu_j}{\sqrt{1-u_j^2}}\quad i=1,\ldots,N_x,\ \ j=1,\ldots,N_v$$

and

$$\lambda=\left(\sum_{i,j}\bar{g}^0_{i,j}\frac{c}{(1-u_j^2)^{3/2}}\Delta u\Delta x_0\right)\Big/\left(\varepsilon\sum_k h(x_k)\right).$$

Here x_k is a point on the Poisson mesh and ε is the width of the grid on the Poisson mesh as described in Section 2.2.6. If $g(x_0,u,t)$ is the solution to (1.21) corresponding to the time interval $[lT_1,(l+1)T_1]$, $l=0,1,\ldots,M-1$ then $g^{l,n}_{i,j}$ is the approximation to $g(x_{0_i},u_j,t_n)$, $n=0,1,2,\ldots,N_g$. At $l=0$, $n=0$ we let $g^{0,0}_{i,j}=\bar{g}^0_{i,j}/\lambda$ so that

$$\sum_{i,j}g^{0,0}_{i,j}\frac{c}{(1-u_j^2)^{3/2}}\Delta u\Delta x_0=\epsilon\sum_k h(x_k).$$

For $l>0$ the initial function for (1.21) is $g(x_0,u,0)=f\left(x_0,\frac{cu}{\sqrt{1-u^2}},lT_1\right)$, with $f(x,v,t)$ the solution to (1.1). In this case the discrete initial function, $g^{l,0}_{i,j}$, is obtained by the procedure described in Section 2.3. That is the solution obtained by the deterministic particle method corresponding to the time interval $[(l-1)T_1,lT_1]$ is reconstructed on the fixed grid on Ω at time lT_1.

2.2.2. The approximation of (1.21)

The approximate solution to (1.21) corresponding to the interval $[lT_1,(l+1)T_1]$ is denoted $g^{l,n}_{i,j}$, $n=0,1,\ldots,N_g$. For $n=0$ then $g^{l,0}_{i,j}$ is obtained in Section 2.2.1. For $t_n\in[0,T_1]$ let $a(i,j,t_n)$, $b(i,j,t_n)$, $c(i,j,t_n)$, $d(i,j,t_n)$ be approximations to the coefficients $a(x_{0_i},v_{0_j},t_n),b(x_{0_i},v_{0_j},t_n),c(x_{0_i},v_{0_j},t_n),d(x_{0_i},v_{0_j},t_n)$ in (1.21). For simplicity we let $g^{l,n}_{i,j}=g^n_{i,j}$ then given $g^n_{i,j}$ to get $g^{n+1}_{i,j}$ we compute as follows. Let

$$s_j=\frac{(1-u_j^2)^{3/2}}{c},\quad s_j^0=\frac{(1-(u_j-0.5\Delta u)^2)^{3/2}}{c},\quad s_j^1=\frac{(1-(u_j+0.5\Delta u)^2)^{3/2}}{c}.$$

The quantity $\frac{(1-u^2)^{3/2}}{c}\frac{\partial}{\partial u}\left(\frac{(1-u^2)^{3/2}}{c}\frac{\partial g}{\partial u}\right)$ is approximated by

$$s_j\left[s_j^1\frac{(g_{i,j+1}-g_{i,j})}{\Delta u}-s_j^0\frac{(g_{i,j}-g_{i,j-1})}{\Delta u}\right]/\Delta u=s_j\frac{[s_j^1g_{i,j+1}-(s_j^1+s_j^0)g_{i,j}+s_j^0g_{i,j-1}]}{(\Delta u)^2}.$$

Then $\bar{g}^{n+1}_{i,j}$ is obtained as a solution to the semi-implicit difference equation

$$\bar{g}_{i,j}^{n+1} = g_{i,j}^{n} + q\Delta t\left[a(i,j,t_n)^2\left(\frac{\bar{g}_{i+1,j}^{n+1} - 2\bar{g}_{i,j}^{n+1} + \bar{g}_{i-1,j}^{n+1}}{(\Delta x_0)^2}\right)\right.$$
$$- 2a(i,j,t_n)b(i,j,t_n)s_j\left(\frac{g_{i+1,j+1}^{n} - g_{i+1,j-1}^{n} - g_{i-1,j+1}^{n} + g_{i-1,j-1}^{n}}{(2\Delta x_0)(2\Delta u)}\right)$$
$$+ b(i,j,t_n)^2 s_j \frac{(s_j^1\bar{g}_{i,j+1}^{n+1} - (s_j^1 + s_j^0)\bar{g}_{i,j}^{n+1} + s_j^0\bar{g}_{i,j-1}^{n+1})}{(\Delta u)^2}$$
$$\left. + c(i,j,t_n)\frac{(g_{i+1,j}^{n} - g_{i-1,j}^{n})}{2\Delta x_0} + d(i,j,t_n)s_j\frac{(g_{i,j+1}^{n} - g_{i,j-1}^{n})}{2\Delta u}\right]. \tag{2.3}$$

If $i = 1$ then $\bar{g}_{i-1,j}^{n+1} = \bar{g}_{N_x,j}^{n+1}$, if $i = N_x$ then $\bar{g}_{i+1,j}^{n+1} = \bar{g}_{1,j}^{n+1}$ which is the periodic boundary condition in x_0. If $j = 1$ then in $\bar{g}_{i,j-1}^{n+1} = 0$ and if $j = N_v$ then $\bar{g}_{i,j+1}^{n+1} = 0$ which is the zero boundary condition at $u = \pm 1$.

One way to solve (2.3) for $\bar{g}_{i,j}^{n+1}$ given that $g_{i,j}^{n}$ is known is to use an iterative procedure. Let $r_1 = \Delta t/(\Delta x_0)^2$, $r_2 = \Delta t/(\Delta u)^2$, $p_1 = \Delta t/(2\Delta x_0)$, $p_2 = \Delta t/(2\Delta u)$, and let $a_{i,j} = a(i,j,t_n)$ and similarly for $b_{i,j}$, $c_{i,j}$, $d_{i,j}$. Then (2.3) is written

$$(1 + 2qr_1a_{i,j}^2 + qr_2b_{i,j}^2(s_j^1 + s_j^0))\bar{g}_{i,j}^{n+1} = qr_1a_{i,j}^2(\bar{g}_{i+1,j}^{n+1} + \bar{g}_{i-1,j}^{n+1}) + qr_2b_{i,j}^2s_j(s_j^1\bar{g}_{i,j+1}^{n+1} + s_j^0\bar{g}_{i,j-1}^{n+1}) + F_{i,j}^{n},$$

where

$$F_{i,j}^{n} = g_{i,j}^{n} - \frac{1}{2}q\sqrt{r_1r_2}a_{i,j}b_{i,j}s_j(g_{i+1,j+1}^{n} - g_{i+1,j-1}^{n} - g_{i-1,j+1}^{n} + g_{i-1,j-1}^{n}) + qp_1c_{i,j}(g_{i+1,j}^{n} - g_{i-1,j}^{n})$$
$$+ qp_2d_{i,j}s_j(g_{i,j+1}^{n} - g_{i,j-1}^{n}).$$

Let $D_{i,j} = 1 + 2qr_1a_{i,j}^2 + qr_2b_{i,j}^2s_j(s_j^1 + s_j^0)$ then

$$\bar{g}_{i,j}^{n+1} = \frac{qr_1a_{i,j}^2}{D_{i,j}}(\bar{g}_{i+1,j}^{n+1} + \bar{g}_{i-1,j}^{n+1}) + \frac{qr_2b_{i,j}^2}{D_{i,j}}s_j(s_j^1\bar{g}_{i,j+1}^{n+1} + s_j^0\bar{g}_{i,j-1}^{n+1}) + \frac{1}{D_{i,j}}F_{i,j}^{n}. \tag{2.4}$$

Given $g_{i,j}^{n}$, that determines $F_{i,j}^{n}$ then (2.4) can be solved iteratively to obtain for $\bar{g}_{i,j}^{n+1}$. Let $h_{i,j}^{0} = g_{i,j}^{n}$. Then for $k = 0, 1, 2, \ldots$

$$h_{i,j}^{k+1} = \frac{qr_1a_{i,j}^2}{D_{i,j}}(h_{i+1,j}^{k} + h_{i-1,j}^{k}) + \frac{qr_2b_{i,j}^2}{D_{i,j}}s_j(s_j^1h_{i,j+1}^{k} + s_j^0h_{i,j-1}^{k}) + \frac{1}{D_{i,j}}F_{i,j}^{n}. \tag{2.5}$$

The above iterative procedure referred to as the Jacobi method is convergent. In fact

$$|h_{i,j}^{k+1} - h_{i,j}^{k}| \leqslant \frac{qr_1a_{i,j}^2}{D_{i,j}}(|h_{i+1,j}^{k} - h_{i+1,j}^{k-1}| + |h_{i-1,j}^{k} - h_{i-1,j}^{k-1}|) + \frac{qr_2b_{i,j}^2}{D_{i,j}}s_j(s_j^1|h_{i,j+1}^{k} - h_{i,j+1}^{k-1}| + s_j^0|h_{i,j-1}^{k} - h_{i,j-1}^{k-1}|).$$

Letting $\|h^k\| = \max_{i,j}|h_{i,j}^{k}|$ and

$$\Theta(t_n) = \max_{i,j}\left(\frac{2qr_1a_{i,j}^2 + qr_2b_{i,j}^2s_j(s_j^1 + s_j^0)}{D_{i,j}}\right),$$

then

$$\|h^{k+1} - h^{k}\| \leqslant \Theta(t_n)\|h^{k} - h^{k-1}\|.$$

Since $0 < \Theta(t_n) < 1$ the sequence $\{h_{i,j}^{k}\}$ converges uniformly in i,j and $\lim_{k\to\infty}h_{i,j}^{k} = \bar{g}_{i,j}^{n+1}$.

The method used to accelerate the convergence rate of the iterative procedure (2.5) is SOR (successive overrelaxation). Here the updated value of $h_{i,j}$ is used in the iterative procedure as soon as it is available.

In addition an extrapolation is carried out based on the updated $h_{i,j}$ and its previous value. Thus for $i > 1$ and $j > 1$ instead of (2.5) we compute

$$\bar{h}_{i,j}^{k+1} = \frac{qr_1a_{i,j}^2}{D_{i,j}}(h_{i+1,j}^k + h_{i-1,j}^{k+1}) + \frac{qr_2b_{i,j}^2}{D_{i,j}}s_j(s_j^1 h_{i,j+1}^k + s_j^0 h_{i,j-1}^{k+1}) + \frac{1}{D_{i,j}}F_{i,j}^n \tag{2.6}$$

and

$$h_{i,j}^{k+1} = \omega\bar{h}_{i,j}^{k+1} + (1-\omega)h_{i,j}^k, \tag{2.7}$$

with $\omega > 1$. A precise determination of the overrelaxation parameter, ω, is based on the eigenvalues, λ, that satisfy

$$\frac{qr_1a_{i,j}^2}{D_{i,j}}(h_{i+1,j} + h_{i-1,j}) + \frac{qr_2b_{i,j}^2}{D_{i,j}}s_j(s_j^1 h_{i,j+1} + s_j^0 h_{i,j-1}) = \lambda h_{i,j}. \tag{2.8}$$

For $\lambda_{\max}$ the maximal eigenvalue then following the theory in [2] the optimal ω is determined through the formula

$$\omega_b = \frac{2}{1+\sqrt{1-\lambda_{\max}^2}}.$$

We determine computationally that $\Theta(t_n)$ can be a good approximation to $\lambda_{\max}$ so for present purposes the optimal ω is computed as

$$\omega_b = \frac{2}{1+\sqrt{1-\Theta(t_n)^2}}.$$

A direct method that can be used for solving (2.3) is the Douglas–Rachford method as described in [16]. Let $r_1 = \Delta t/(\Delta x_0)^2$, $r_2 = \Delta t/(\Delta u)^2$, $p_1 = \Delta t/(2\Delta x_0)$, $p_2 = \Delta t/(2\Delta u)$, and

$$\delta_x^2 g_{i,j} = g_{i+1,j} - 2g_{i,j} + g_{i-1,j}, \quad \delta_u^2 g_{i,j} = s_j s_j^1 g_{i,j+1} - s_j(s_j^1 + s_j^0)g_{i,j} + s_j s_j^0 g_{i,j-1},$$
$$\delta_{0,x} g_{i,j} = g_{i+1,j} - g_{i-1,j}, \quad \delta_{0,u} g_{i,j} = s_j(g_{i,j+1} - g_{i,j-1}),$$

$a_{i,j} = a(i,j,t_n)$ and similarly for $b_{i,j}$, $c_{i,j}$, $d_{i,j}$. The difference equation is written

$$(1 - qa_{i,j}^2 r_1\delta_x^2 - qb_{i,j}^2 r_2\delta_u^2)\bar{g}_{i,j}^{n+1} = \left(1 - \frac{1}{2}qa_{i,j}b_{i,j}\sqrt{r_1r_2}\delta_{0,x}\delta_{0,u} + qc_{i,j}p_1\delta_{0,x} + qd_{i,j}p_2\delta_{0,u}\right)g_{i,j}^n. \tag{2.9}$$

Eq. (2.9) is replaced by

$$(1 - qa_{i,j}^2 r_1\delta_x^2)(1 - qb_{i,j}^2 r_2\delta_u^2)\bar{g}_{i,j}^{n+1} = \left(1 + q^2a_{i,j}^2b_{i,j}^2 r_1r_2\delta_x^2\delta_u^2 - \frac{1}{2}qa_{i,j}b_{i,j}\sqrt{r_1r_2}\delta_{0,x}\delta_{0,u} + qc_{i,j}p_1\delta_{0,x} + qd_{i,j}p_2\delta_{0,u}\right)g_{i,j}^n. \tag{2.10}$$

Effectively the term $q^2a_{i,j}^2b_{i,j}^2r_1r_2\delta_x^2\delta_u^2\bar{g}_{i,j}^{n+1}$ is added to the left side of (2.9) and is balanced by the term $q^2a_{i,j}^2b_{i,j}^2r_1r_2\delta_x^2\delta_u^2 g_{i,j}^n$ added to the right side of the equation. Eq. (2.10) is equivalent to

$$(1 - qa_{i,j}^2 r_1\delta_x^2)g_{i,j}^* = \left(1 + qb_{i,j}^2 r_2\delta_u^2 - \frac{1}{2}qa_{i,j}b_{i,j}\sqrt{r_1r_2}\delta_{0,x}\delta_{0,u} + qc_{i,j}p_1\delta_{0,x} + qd_{i,j}p_2\delta_{0,u}\right)g_{i,j}^n, \tag{2.11}$$

$$(1 - qb_{i,j}^2 r_2\delta_u^2)\bar{g}_{i,j}^{n+1} = g_{i,j}^* - qb_{i,j}^2 r_2\delta_u^2 g_{i,j}^n. \tag{2.12}$$

Thus given $g_{i,j}^n$ to get $\bar{g}_{i,j}^{n+1}$ one solves (2.11) in the index i for each j to obtain the array $g_{i,j}^*$. Then (2.12) is solved in the index j for each i to obtain $\bar{g}_{i,j}^{n+1}$.

According to (1.5) the solution to (1.1) satisfies

$$\int_0^L \int_{-\infty}^{\infty} f(x,v,t)\mathrm{d}v\,\mathrm{d}x = \int_0^L h(x)\mathrm{d}x.$$

In terms of the solution to (1.21) this condition is

$$\int_0^L \int_{-1}^{1} g(x_0,u,t)\frac{c}{(1-u^2)^{3/2}}\,\mathrm{d}u\,\mathrm{d}x_0 = \int_0^L h(x_0)\mathrm{d}x_0.$$

Thus in the discrete method we let

$$\lambda = \left(\sum_{i,j}\frac{c}{(1-u_j^2)^{3/2}}\bar{g}_{i,j}^{n+1}\Delta x_0\Delta u\right)\Big/\left(\epsilon\sum_k h(x_k)\right)$$

and then $g_{i,j}^{n+1} = g_{i,j}^{l,n+1} = \bar{g}_{i,j}^{n+1}/\lambda$ so that

$$\sum_{i,j} g_{i,j}^{l,n+1}\frac{c}{(1-u_j^2)^{3/2}}\Delta u\Delta x_0 = \epsilon\sum_k h(x_k). \tag{2.13}$$

The purpose for the renormalization of $g_{i,j}^{l,n}$ is to maintain Eq. (2.13) at each step so as to preserve charge neutrality in the approximation of the Poisson equation.

For relatively small q the more efficient method for approximating the solution to (1.21) is the iterative procedure (SOR) rather than the direct method. This is because decreasing q decreases the value $\Theta(t_n)$ which governs the rate of convergence of the iterative procedure. Thus for small values of q the SOR method converges to a desired degree of accuracy with relatively few iterations. For the computations of Section 3 the SOR method is used. The iteration sequence is stopped when $\|h^k - h^{k-1}\| \leqslant \gamma$ with $\gamma = 10^{-8}$ to 10^{-11} depending on the computation.

2.2.3. Approximation of (1.24) and (1.25), particle trajectories

For $t_n \in [0,T_1]$ let $(x(x_{0_i},v_{0_j},t_n),v(v_{0_i},v_{0_j},t_n))$, $v_{0_j} = cu_j/\left(\sqrt{1-u_j^2}\right)$ be the solution to (1.24) and (1.25) at time t_n with initial point (x_{0_i},v_{0_j}). The approximation to this trajectory is denoted $x(i,j,t_n)$,$v(i,j,t_n)$. The approximation to the electric field $E(x(x_{0_i},v_{0_j},t_n),t_n)$ is denoted $\overline{E}(x(i,j,t_n),t_n)$. Then at time t_n given $x(i,j,t_n)$,$v(i,j,t_n)$ and $\overline{E}(x(i,j,t_n),t_n)$ to get $x(i,j,t_{n+1})$,$v(i,j,t_{n+1})$ we solve for $t_n \leqslant t \leqslant t_{n+1}$

$$\frac{\mathrm{d}x}{\mathrm{d}t} = v, \quad x(t_n) = x(i,j,t_n), \tag{2.14}$$

$$\frac{\mathrm{d}v}{\mathrm{d}t} = \overline{E}(x(i,j,t_n),t_n) - \beta v, \quad v(t_n) = v(i,j,t_n). \tag{2.15}$$

Equivalently we can solve for $0 \leqslant t \leqslant \Delta t$

$$\frac{\mathrm{d}\tilde{x}}{\mathrm{d}t} = \tilde{v}, \quad \tilde{x}(0) = x(i,j,t_n), \tag{2.16}$$

$$\frac{\mathrm{d}\tilde{v}}{\mathrm{d}t} = \overline{E}(x(i,j,t_n),t_n) - \beta\tilde{v}, \quad \tilde{v}(0) = v(i,j,t_n). \tag{2.17}$$

Then $x(i,j,t_{n+1}) = \tilde{x}(\Delta t)$, $v(i,j,t_{n+1}) = \tilde{v}(\Delta t)$. The solution to (2.16) and (2.17) is

$$\tilde{x}(\Delta t) = x(i,j,t_n) + \frac{(1-\mathrm{e}^{-\beta\Delta t})}{\beta}v(i,j,t_n) + \left(\frac{\Delta t}{\beta} - \frac{(1-\mathrm{e}^{-\beta\Delta t})}{\beta^2}\right)\overline{E}(x(i,j,t_n),t_n),$$

$$\tilde{v}(\Delta t) = \mathrm{e}^{-\beta\Delta t} v(i,j,t_n) + \frac{(1-\mathrm{e}^{-\beta\Delta t})}{\beta}\overline{E}(x(i,j,t_n),t_n).$$

Therefore, to obtain particle trajectories let $x(i,j,0) = x_{0_i},\ v(i,j,0) = v_{0_j}$. Then given $x(i,j,t_n)$, $v(i,j,t_n)$, and $\overline{E}(x(i,j,t_n),t_n)$ quantities at time t_{n+1} are

$$x(i,j,t_{n+1}) = x(i,j,t_n) + \frac{(1-\mathrm{e}^{-\beta\Delta t})}{\beta} v(i,j,t_n) + \left(\frac{\Delta t}{\beta} - \frac{(1-\mathrm{e}^{-\beta\Delta t})}{\beta^2}\right)\overline{E}(x(i,j,t_n),t_n), \tag{2.18}$$

$$v(i,j,t_{n+1}) = \mathrm{e}^{-\beta\Delta t} v(i,j,t_n) + \frac{(1-\mathrm{e}^{-\beta\Delta t})}{\beta}\overline{E}(x(i,j,t_n),t_n). \tag{2.19}$$

2.2.4. Approximation of (1.28)–(1.31), coefficients a(i,j,t_n), b(i,j,t_n)

Along the trajectory $x(x_{0_i}, v_{0_j}, t),\ v(x_{0_i}, v_{0_j}, t),\ v_{0_j} = cu_j/\left(\sqrt{1-u_j^2}\right)$, the solution to (1.28) and (1.29) is denoted $\frac{\partial x}{\partial v_0}(x_{0_i}, v_{0_j}, t)$, $\frac{\partial v}{\partial v_0}(x_{0_i}, v_{0_j}, t)$. The approximations to these quantities at time $t_n \in [0,T_1]$ are denoted $\frac{\partial x}{\partial v_0}(i,j,t_n)$, $\frac{\partial v}{\partial v_0}(i,j,t_n)$ and similarly for $\frac{\partial x}{\partial x_0}(i,j,t_n)$, $\frac{\partial v}{\partial x_0}(i,j,t_n)$. The equations for the approximate first partial derivatives are obtained by differentiating (2.18) and (2.19) with respect to x_0 and v_0. The coefficients $a(i,j,t_n)$, $b(i,j,t_n)$ are therefore obtained as follows: at t_n=0

$$\frac{\partial x}{\partial x_0}(i,j,0) = 1, \quad \frac{\partial v}{\partial x_0}(i,j,0) = 0, \quad \frac{\partial x}{\partial v_0}(i,j,0) = 0, \quad \frac{\partial v}{\partial v_0}(i,j,0) = 1,$$

$$a(i,j,0) = \frac{\partial x}{\partial v_0}(i,j,0), \quad b(i,j,0) = \frac{\partial x}{\partial x_0}(i,j,0).$$

Then given values of $\frac{\partial x}{\partial x_0}(i,j,t_n)$, $\frac{\partial v}{\partial x_0}(i,j,t_n)$, $\frac{\partial x}{\partial v_0}(i,j,t_n)$, $\frac{\partial v}{\partial v_0}(i,j,t_n)$ quantities at time t_{n+1} are computed by

(i)
$$\frac{\partial x}{\partial x_0}(i,j,t_{n+1}) = \frac{\partial x}{\partial x_0}(i,j,t_n) + \frac{(1-\mathrm{e}^{-\beta\Delta t})}{\beta}\frac{\partial v}{\partial x_0}(i,j,t_n) + \left(\frac{\Delta t}{\beta} - \frac{(1-\mathrm{e}^{-\beta\Delta t})}{\beta^2}\right)\frac{\partial \overline{E}}{\partial x} \times (x(i,j,t_n),t_n)\frac{\partial x}{\partial x_0}(i,j,t_n), \tag{2.20}$$

(ii)
$$\frac{\partial v}{\partial x_0}(i,j,t_{n+1}) = \mathrm{e}^{-\beta\Delta t}\frac{\partial v}{\partial x_0}(i,j,t_n) + \frac{(1-\mathrm{e}^{-\beta\Delta t})}{\beta}\frac{\partial \overline{E}}{\partial x}(x(i,j,t_n),t_n)\frac{\partial x}{\partial x_0}(i,j,t_n), \tag{2.21}$$

(iii)
$$\frac{\partial x}{\partial v_0}(i,j,t_{n+1}) = \frac{\partial x}{\partial v_0}(i,j,t_n) + \frac{(1-\mathrm{e}^{-\beta\Delta t})}{\beta}\frac{\partial v}{\partial v_0}(i,j,t_n) + \left(\frac{\Delta t}{\beta} - \frac{(1-\mathrm{e}^{-\beta\Delta t})}{\beta^2}\right)\frac{\partial \overline{E}}{\partial x} \times (x(i,j,t_n),t_n)\frac{\partial x}{\partial v_0}(i,j,t_n), \tag{2.22}$$

(iv)
$$\frac{\partial v}{\partial v_0}(i,j,t_{n+1}) = -\mathrm{e}^{-\beta\Delta t}\frac{\partial v}{\partial v_0}(i,j,t_n) + \frac{(1-\mathrm{e}^{-\beta\Delta t})}{\beta}\frac{\partial \overline{E}}{\partial x}(x(i,j,t_n),t_n)\frac{\partial x}{\partial v_0}(i,j,t_n) \tag{2.23}$$

and

$$a(i,j,t_{n+1}) = \mathrm{e}^{\beta t_{n+1}}\frac{\partial x}{\partial v_0}(i,j,t_{n+1}), \quad b(i,j,t_{n+1}) = \mathrm{e}^{\beta t_{n+1}}\frac{\partial x}{\partial x_0}(i,j,t_{n+1}).$$

The quantity $\frac{\partial \overline{E}}{\partial x}(x,t_n)$ is defined in Section 2.2.6.

2.2.5. The approximation of (1.32) and (1.33), coefficients $c(i,j,t_n)$, $d(i,j,t_n)$

Along the trajectory $x(x_{0_i}, v_{0_j}, t)$, $v(x_{0_i}, v_{0_j}, t)$, $v_{0_j} = cu_j/\left(\sqrt{1-u_j^2}\right)$, the solution to (1.32) and (1.33) is denoted $\frac{\partial^2 x}{\partial x_0^s\,\partial v_0^r}(x_{0_i}, v_{0_j}, t)$, $\frac{\partial^2 v}{\partial x_0^s\,\partial v_0^r}(x_{0_i}, v_{0_j}, t)$. The approximations to these quantities at time $t \in [0, T_1]$ are denoted $\frac{\partial^2 x}{\partial x_0^s\,\partial v_0^r}(i,j,t_n)$, $\frac{\partial^2 x}{\partial x_0^s\,\partial v_0^r}(i,j,t_n)$. The equations for the second partial derivatives are obtained by taking second derivatives of (2.18) and (2.19) with respect to x_0, v_0. Thus, let

$$\frac{\partial^2 x}{\partial x_0^s\,\partial v_0^r}(i,j,0) = 0, \quad \frac{\partial^2 x}{\partial x_0^s\,\partial v_0^r}(i,j,0) = 0, \quad c(i,j,0) = 0, \quad d(i,j,0) = 0.$$

Then given quantities at time t_n quantities at time t_{n+1} are computed by

$$\begin{aligned}(\mathrm{i}) \quad \frac{\partial^2 x}{\partial x_0^s\,\partial v_0^r}(i,j,t_{n+1}) &= \frac{\partial^2 x}{\partial x_0^s\,\partial v_0^r}(i,j,t_n) + \frac{(1-\mathrm{e}^{-\beta\Delta t})}{\beta}\frac{\partial^2 v}{\partial x_0^s\,\partial v_0^r}(i,j,t_n) \\ &\quad + \left(\frac{\Delta t}{\beta} - \frac{(1-\mathrm{e}^{-\beta\Delta t})}{\beta^2}\right)\frac{\partial \overline{E}}{\partial x}(x(i,j,t_n),t_n)\frac{\partial^2 x}{\partial x_0^s\,\partial v_0^r}(i,j,t_n) \\ &\quad + \left(\frac{\Delta t}{\beta} - \frac{(1-\mathrm{e}^{-\beta\Delta t})}{\beta^2}\right)\frac{\partial^2 \overline{E}}{\partial x^2}(x(i,j,t_n),t_n)\left(\frac{\partial x}{\partial x_0}\right)^s\left(\frac{\partial x}{\partial v_0}\right)^r(i,j,t_n), \end{aligned} \tag{2.24}$$

$$\begin{aligned}(\mathrm{ii}) \quad \frac{\partial^2 v}{\partial x_0^s\,\partial v_0^r}(i,j,t_{n+1}) &= \mathrm{e}^{-\beta\Delta t}\frac{\partial^2 v}{\partial x_0^s\,\partial v_0^r}(i,j,t_n) + \frac{(1-\mathrm{e}^{-\beta\Delta t})}{\beta}\frac{\partial \overline{E}}{\partial x}(x(i,j,t_n),t_n)\frac{\partial^2 x}{\partial x_0^s\,\partial v_0^r}(i,j,t_n) \\ &\quad + \frac{(1-\mathrm{e}^{-\beta\Delta t})}{\beta}\frac{\partial^2 \overline{E}}{\partial x^2}(x(i,j,t_n),t_n)\left(\frac{\partial x}{\partial x_0}\right)^s\left(\frac{\partial x}{\partial v_0}\right)^r(i,j,t_n), \end{aligned} \tag{2.25}$$

$r, s = 0, 1, 2, \;\; r + s = 2$

and

$$c(i,j,t_{n+1}) = \mathrm{e}^{3\beta t_{n+1}}\left(\frac{\partial v}{\partial v_0}P_1 - \frac{\partial x}{\partial v_0}P_2\right)(i,j,t_{n+1}),$$

$$d(i,j,t_{n+1}) = \mathrm{e}^{3\beta t_{n+1}}\left(\frac{\partial x}{\partial x_0}P_2 - \frac{\partial v}{\partial x_0}P_1\right)(i,j,t_{n+1}),$$

where

$$P_1 = \left[-\frac{\partial^2 x}{\partial x_0^2}\left(\frac{\partial x}{\partial v_0}\right)^2 + 2\frac{\partial^2 x}{\partial x_0\,\partial v_0}\left(\frac{\partial x}{\partial v_0}\right)\left(\frac{\partial x}{\partial x_0}\right) - \frac{\partial^2 x}{\partial v_0^2}\left(\frac{\partial x}{\partial x_0}\right)^2\right](i,j,t_{n+1}),$$

$$P_2 = \left[-\frac{\partial^2 v}{\partial x_0^2}\left(\frac{\partial x}{\partial v_0}\right)^2 + 2\frac{\partial^2 v}{\partial x_0\,\partial v_0}\left(\frac{\partial x}{\partial v_0}\right)\left(\frac{\partial x}{\partial x_0}\right) - \frac{\partial^2 v}{\partial v_0^2}\left(\frac{\partial x}{\partial x_0}\right)^2\right](i,j,t_{n+1}).$$

The quantity $\frac{\partial^2 \overline{E}}{\partial x^2}(x,t_n)$ is defined in Section 2.2.6.

2.2.6. The approximation of the charge density and electric field

An approximate trajectory $x(i,j,t_n)$, $v(i,j,t_n)$, $t_n \in [0,T_1]$, $n = 0, 1, 2, \ldots, N_g$ can be considered the path of an element of charge, $q_{i,j}$, in phase space. This element of charge can be defined as $q_{i,j} = \bar{f}(x(i,j,t_n), v(i,j,t_n), t_n)\Delta A_{i,j}$ where $\bar{f}$ is the approximate distribution function and $\Delta A_{i,j}$ is a differential area of phase space associated with the i,j trajectory at time t_n. In terms of the differential of area in x_0, u space then

$$\Delta A_{i,j} \approx \frac{c}{(1-u_j^2)^{3/2}} \exp(-\beta t_n)\Delta x_0 \Delta u.$$

Also on the time intervals $[lT_1,(l+1)T_1]$, $l = 0,1,\ldots,M-1$

$$\bar{f}(x(i,j,t_n), v(i,j,t_n), t_n) = \exp(\beta t_n) g_{i,j}^{l,n}.$$

Thus

$$q_{i,j}^{l,n} = \exp(\beta t_n) g_{i,j}^{l,n} \frac{c}{(1-u_j^2)^{3/2}} \exp(-\beta t_n)\Delta x_0 \Delta u = \frac{c g_{i,j}^{l,n}}{(1-u_j^2)^{3/2}} \Delta x_0 \Delta u. \tag{2.26}$$

It is convenient to define a discrete charge density as

$$\tilde{\rho}(x,t_n) = \sum_{i,j} q_{i,j}^{l,n} \delta(x - x(i,j,t_n)) - h(x),$$

where $\delta(x)$ is the Dirac delta function.

We approximate the solution to

$$\frac{\partial^2 \phi}{\partial x^2} = \rho(x,t), \quad \phi(0,t) = \phi(L,t) = 0$$

by the particle-in-cell method. Let N_p be a positive integer and $\epsilon = L/N_P$. The interval $[0,L]$ is then partitioned as $x_k = k\epsilon$, $k = 0, 1, \ldots, N_p$ which gives a uniform grid of width ϵ. Then let $w(x)$ be a continuous function with compact support such that

$$\int_{-\infty}^{\infty} w(x)\mathrm{d}x = 1, \quad \sum_{i \in z} w(x-i) = 1,\ z - \text{integers}$$

and set $w_\epsilon(x) = \frac{1}{\epsilon} w\left(\frac{x}{\epsilon}\right)$. The grid charge density $\rho_k(t_n)$, $k = 0, \ldots, N_p$ is then determined as follows: if supp $w_\epsilon(x - x_k) \in [0,L]$ then

$$\rho_k(t_n) = \int_0^L w_\epsilon(x - x_k)\tilde{\rho}(x,t_n)\mathrm{d}x = \sum_{i,j} q_{i,j}^{l,n} w_\epsilon(x(i,j,t_n) - x_k) - h(x_k).$$

Near the endpoints of the interval this formula is modified according to the periodicity of the solution. Given the normalization of $g_{i,j}^{l,n}$ previously described it follows that $\epsilon \sum_k \rho_k(t_n) = 0$.

For the potential at the grid points we solve

$$\frac{\phi_{k+1} - 2\phi_k + \phi_{k-1}}{\epsilon^2} = \rho_k(t_n), \quad k = 1, \ldots, N_p - 1,$$

$$\phi_0 = 0, \quad \phi_{N_p} = 0.$$

The electric field at the grid points, x_k, for $k = 1, \ldots, N_p - 1$ is obtained as

$$E_k(t_n) = \frac{\phi_{k+1} - \phi_{k-1}}{2\epsilon}.$$

For the problems we study it can be determined analytically that $E(0,t) = E(L,t) = 0$. Therefore, for $k = 0$ and $k = N_p$ we set $E_0(t_n) = E_{N_p}(t_n) = 0$. We also compute

$$DE_k(t_n) = \frac{E_{k+1}(t_n) - E_{k-1}(t_n)}{2\epsilon}, \quad D^2 E_k(t_n) = \frac{E_{k+1}(t_n) - 2E_k(t_n) + E_{k-1}(t_n)}{\epsilon^2}.$$

The approximate field $\overline{E}(x,t_n)$ and its derivatives are then defined as continuous functions of x

$$\overline{E}(x,t_n) = \epsilon \sum_{k=0}^{N_p} E_k(t_n) w_\epsilon(x - x_k), \tag{2.27}$$

$$\frac{\partial \overline{E}}{\partial x}(x,t_n) = \epsilon \sum_{k=0}^{N_p} DE_k(t_n) w_\epsilon(x - x_k), \tag{2.28}$$

$$\frac{\partial^2 \overline{E}}{\partial x^2}(x,t_n) = \epsilon \sum_{k=0}^{N_p} D^2E_k(t_n) w_\epsilon(x - x_k). \tag{2.29}$$

A particular function $w(x)$ used in the present computation is

$$w(x) = \begin{cases} \frac{1}{2}\left(\frac{3}{2} + x\right)^2, & -\frac{3}{2} \leqslant x \leqslant -\frac{1}{2}, \\ \frac{3}{4} - x^2, & -\frac{1}{2} \leqslant x \leqslant \frac{1}{2}, \\ \frac{1}{2}\left(\frac{3}{2} - x\right)^2, & \frac{1}{2} \leqslant x \leqslant \frac{3}{2}, \\ 0, & |x| > \frac{3}{2}. \end{cases}$$

The function $w(x)$ is of class C^1.

2.3. Regriding the solution

At times $\tau_{l+1} = (l+1)T_1$, $l = 0, 1, \ldots, M-1$ the solution along particle trajectories is interpolated onto the fixed grid given by (2.1). We set $t_n = 0$, and the particle method is restarted with the initial data being the interpolated solution at time τ_{l+1}. The regriding is carried out so as to preserve the total charge, momentum, and kinetic energy of the solution. Our method for doing this is motivated by the procedure in [13]. At time $\tau_{l+1} = lT_1 + t_{N_g} = (l+1)T_1$ the i',j' trajectory has coordinates in phase space given by $(x(i',j',t_{N_g})), v(i',j',t_{N_g})$. These coordinates in phase space correspond to coordinates (x_p,u_p) in Ω where $x_p = x(i',j',t_{N_g})$ and $u_p = v(i',j',t_{N_g})/\sqrt{c^2 + v(i',j',t_{N_g})^2}$. The charge along the i',j' trajectory is given by (2.26) and is $q^{l,N_g}_{i',j'}$. Referring to the partition of Ω given by (2.1) we assume indices i and j such that $x_{0_i} \leqslant x_p \leqslant x_{0_{i+1}}$ and $u_j \leqslant u_p \leqslant u_{j+1}$ with (x_{0_i}, u_j) a grid point given by (2.1). Corresponding to (x_{0_i}, u_j), in Ω is the point (x_{0_i}, v_{0_j}) in A_0 where $v_{0_j} = cu_j/(\sqrt{1-u_j^2})$. The charge $q^{l,N_g}_{i',j'}$ is distributed between the eight grid points with indices $(i,j-1)$, (i,j), $(i,j+1)$, $(i,j+2)$, $(i+1,j-1)$, $(i+1,j)$, $(i+1,j+1)$, $(i+1,j+2)$. Let $\alpha_{i,j}(i',j')$ be the charge contributed to the i,j grid point in Ω from the charge $q^{l,N_g}_{i',j'}$. We determine the $\alpha_{i,j}(i',j')$ as follows: let $P_1 = (x_p - x_i)/\Delta x_0$, $P_2 = 1 - P_1$, then $q_L = P_2(q^{l,N_g}_{i',j'})$, $q_R = P_1(q^{l,N_g}_{i',j'})$. Thus q_L is charge distributed to the left of x_p and q_R is charge distributed to the right of x_p. Let $z_L = q_L/2$ and y_1, y_2, y_3 be the solution to

$$\begin{aligned} &y_1 + y_2 + y_3 = z_L, \\ &v_{0_{j-1}} y_1 + v_{0_j} y_2 + v_{0_{j+1}} y_3 = v(i',j',t_{N_g}) z_L, \\ &(v_{0_{j-1}})^2 y_1 + (v_{0_j})^2 y_2 + (v_{0_{j+1}})^2 y_3 = (v(i',j',t_{N_g}))^2 z_L \end{aligned} \tag{2.30}$$

and z_1, z_2, z_3 be the solutions to

$$\begin{aligned} &z_1 + z_2 + z_3 = z_L, \\ &v_{0_j} z_1 + v_{0_{j+1}} z_2 + v_{0_{j+2}} z_3 = v(i',j',t_{N_g}) z_L, \\ &(v_{0_j})^2 z_1 + (v_{0_{j+1}})^2 z_2 + (v_{0_{j+2}})^2 z_3 = (v(i',j',t_{N_g}))^2 z_L. \end{aligned} \tag{2.31}$$

The charge distributed to points in Ω with coordinates (x_{0_i}, u_k), $k = j-1, \ldots, j+2$ is

$$\alpha_{i,j-1}(i',j') = y_1, \quad \alpha_{i,j}(i',j') = y_2 + z_1, \quad \alpha_{i,j+1}(i',j') = y_3 + z_2, \quad \alpha_{i,j+2}(i',j') = z_3. \tag{2.32}$$

The charge distributed to points in Ω with coordinates $(x_{0_{i+1}}, u_k)$, $k = j-1, \ldots, j+2$ is obtained by replacing z_L in Eqs. (2.30) and (2.31) with $z_R = q_R/2$ and computing the y_1, y_2, y_3, z_1, z_2, z_3 accordingly. Then replacing i with $i+1$ in Eqs. (2.32) we obtain $\alpha_{i+1,j-1}(i',j')$, $\alpha_{i+1,j}(i',j')$, $\alpha_{i+1,j+1}(i',j')$, $\alpha_{i+1,j+2}(i',j')$.

Summing over all particle trajectories gives the total charge at the i,j grid point in Ω, that is

$$q_{i,j}^{l+1,0} = \sum_{i',j'} \alpha_{i,j}(i',j').$$

Let $da_j = c\Delta x_0 \Delta_u/(l-u_j^2)^{3/2}$ then $g_{i,j}^{l+1,0} = q_{i,j}^{l+1,0}/da_j$. The grid function $g_{i,j}^{l+1,0}$ is the initial data for (2.3) for the time interval $[(l+1)T_1,(l+2)T_1]$.

One can verify that

$$\sum\nolimits_{i,j} g_{i,j}^{l+1,0} \frac{c\Delta x_0 \Delta u}{(1-u_j^2)^{3/2}} = \sum\nolimits_{i,j} g_{i,j}^{l,N_g} \frac{c\Delta x_0 \Delta u}{(1-u_j^2)^{3/2}},$$

$$\sum\nolimits_{i,j} v_{0_j} g_{i,j}^{l+1,0} \frac{c\Delta x_0 \Delta u}{(1-u_j^2)^{3/2}} = \sum\nolimits_{i,j} v(i,j,t_{N_g}) g_{i,j}^{l,N_g} \frac{c\Delta x_0 \Delta u}{(1-u_j^2)^{3/2}},$$

$$\sum\nolimits_{i,j} (v_{0_j})^2 g_{i,j}^{l+1,0} \frac{c\Delta x_0 \Delta u}{(1-u_j^2)^{3/2}} = \sum\nolimits_{i,j} (v(i,j,t_{N_g}))^2 g_{i,j}^{l,N_g} \frac{c\Delta x_0 \Delta u}{(1-u_j^2)^{3/2}}. \tag{2.33}$$

That is the charge, momentum, and kinetic energy integrals are preserved by the regriding process.

The primary purpose of the regriding of the solution is to improve the long term stability and accuracy of the numerical method. The coefficients $a, \ldots, d$ in (1.21) grow with time. For sufficiently large t the coefficients become large in magnitude, and this causes inaccuracies and instabilities to develop in the numerical method. The solution to this problem is to limit the time interval on which the deterministic particle method is applied. Thus the computed solution is periodically reconstructed on the fixed grid, and the particle method is then restarted with $t_n = 0$.

2.4. The solution on the time interval [0,T]

The quantities used to represent the solution at times $\bar{t} \in [0,T]$ are the electrostatic energy defined as

$$\mathrm{ese}(\bar{t}) = \frac{1}{2}\int_0^L (E(x,\bar{t}))^2 \, \mathrm{d}x, \tag{2.34}$$

the kinetic energy

$$\mathrm{ke}(\bar{t}) = \frac{1}{2}\int_0^L \int_{-\infty}^{\infty} v^2 f(x,v,\bar{t}) \mathrm{d}v \, \mathrm{d}x \tag{2.35}$$

and the free energy defined as

$$\mathrm{FE}(\bar{t}) = \mathrm{ese}(\bar{t}) + \mathrm{ke}(\bar{t}) - q/\beta \mathrm{ent}(\bar{t}), \tag{2.36}$$

where $\mathrm{ent}(\bar{t})$ is the entropy of the system given by

$$\mathrm{ent}(\bar{t}) = -\int_0^L \int_{-\infty}^{\infty} f(x,v,\bar{t}) \ln(f(x,v,\bar{t})) \mathrm{d}v \, \mathrm{d}x.$$

For $\bar{t} \in [lT_1, (l+l)T_1]$ then according to (1.34) $f(x,v,\bar{t})$ has a representation as $f(x,v,\bar{t}) = e^{\beta t} g(x_0(x,v,t), u(v_0(x,v,t)),t)$ with $t \in [0,T_1]$. In terms of the function $g(x_0,u,t)$ and given (1.17) and (1.26) then

$$\mathrm{ke}(\bar{t}) = \frac{1}{2}\int_0^L \int_{-1}^1 (v(x_0, v_0(u), t))^2 g(x_0,u,t) \frac{c}{(1-u^2)^{3/2}}\, \mathrm{d}u\, \mathrm{d}x_0$$

and

$$\mathrm{ent}(\bar{t}) = -\int_0^L \int_{-1}^1 g(x_0,u,t) \ln(e^{\beta t} g(x_0,u,t)) \frac{c}{(1-u^2)^{3/2}}\, \mathrm{d}u\, \mathrm{d}x_0.$$

For discretized versions of these quantities let $\bar{t}_k = \tau_l + t_n$ where $\tau_l = lT_1$, $l = 0, 1, \ldots, M$, $t_n = n\Delta t$, $n = 0, 1, \ldots, N_g$ and $k = lN_g + n$. Then in terms of the discrete trajectories (2.18) and (2.19) and the approximation to (1.21)

$$\mathrm{ke}(\bar{t}_k) = \frac{1}{2}\sum_{i,j} (v(i,j,t_n))^2 g_{i,j}^{l,n} \frac{c}{(1-u_j^2)^{3/2}} \Delta u \Delta x_0, \tag{2.37}$$

$$\mathrm{ent}(\bar{t}_k) = -\sum_{i,j} g_{i,j}^{l,n} \ln(e^{\beta t_n} g_{i,j}^{l,n}) \frac{c}{(1-u_j^2)^{3/2}} \Delta u \Delta x_0. \tag{2.38}$$

To compute the electrostatic energy the particle trajectories given by (2.18) and (2.19) are ordered by the x coordinates as $0 < x_1 \leqslant \cdots \leqslant x_i \cdots \leqslant x_N < L$, $N = N_x \times N_v$. Each x_i represents the position of a particle, $\overline{E}(x_i,t_n)$ is the electric field at the particle position at time $\bar{t}_k = \tau_l + t_n$, and $\Delta x_i = x_{i+1} - x_i$. Then

$$\mathrm{ese}(\bar{t}_k) = \frac{1}{2}\sum_{i=1}^{N-1} \left(\frac{\overline{E}(x_i,t_n) + \overline{E}(x_{i+1},t_n)}{2}\right)^2 \Delta x_i. \tag{2.39}$$

At times $\bar{t}_k = \tau_l$ the solution along trajectories is reconstructed on the fixed grid. At these times the ese, ke, and FE are computed based on the reconstructed solution. So, for example,

$$\mathrm{ke}(\tau_l) = \frac{1}{2}\sum_{i,j} (v_{0_j})^2 g_{i,j}^{l,0} \frac{c}{(1-u_j^2)^{3/2}} \Delta u \Delta x_0.$$

According to (2.33) the reconstructed solution preserves kinetic energy. Thus the ke graph maintains continuity in time. However, the quantities ese and ent are not preserved under the regriding and so the ese and FE graphs can exhibit discontinuities at the regriding points.

2.4.1. Summary of numerical method

Given the time interval $[0,T]$ let $T_1 > 0$ be such that $T/T_1 = M$ an integer. Then for positive integers N_x, N_v, N_g, N_p let $\Delta x_0 = L/N_x$, $\Delta u = 2/(N_v+1)$, $\Delta t = T_1/N_g$, $\varepsilon = L/N_p$. Grid points (x_{0_i}, u_j) and (x_{0_i}, v_{0_j}) are given by

$$x_{0_i} = \left(i - \frac{1}{2}\right)\Delta x_0, \quad i = 1, \ldots, N_x,$$

$$u_j = -1 + j\Delta u, \quad v_{0_j} = \frac{cu_j}{\sqrt{1-u_j^2}}, \quad j = 1, \ldots, N_v.$$

The time interval $[0,T_1]$ is partitioned as $t_n = n\Delta t$, $n = 0, 1, 2, \ldots, N_g$.
The Poisson mesh is given as $x_k = k\epsilon$, $k = 0, 1, \ldots, N_p$.
For $l = 0, 1, \ldots, M$ let $\tau_l = lT_1$ and for $k = lN_g + n$ let $\bar{t}_k = \tau_l + t_n$.

(1) at $l = 0$, $n = 0$, that is, τ_l=0, t_n=0:

$$\bar{g}^0_{i,j} = f_0(x_{0_i}, v_{0_j}) = f\left(x_{0_i}, \frac{cu_j}{\sqrt{1-u_j^2}}\right), \quad \lambda = \left(\sum_{i,j} \bar{g}^0_{i,j} \frac{c}{(1-u_j^2)^{3/2}} \Delta x_0 \Delta u\right) \Big/ \left(\epsilon \sum_k h(x_k)\right)$$

and $g^{0,0}_{i,j} = \bar{g}^0_{i,j}/\lambda$.

(2) at $l \geqslant 0$, $n = 0$, that is, $\tau_l = lT_1$, $t_n = 0$:

$$x(i,j,0) = x_{0_i}, \quad v(i,j,0) = v_{0_j},$$

$$\frac{\partial x}{\partial x_0}(i,j,0) = 1, \quad \frac{\partial v}{\partial x_0}(i,j,0) = 0, \quad \frac{\partial x}{\partial v_0}(i,j,0) = 0, \quad \frac{\partial v}{\partial v_0}(i,j,0) = 1,$$

$$a(i,j,0) = \frac{\partial x}{\partial v_0}(i,j,0) = 0, \quad b(i,j,0) = \frac{\partial x}{\partial x_0}(i,j,0) = 1,$$

$$\frac{\partial^2 x}{\partial x_0^s\, \partial v_0^r}(i,j,0) = 0, \quad \frac{\partial^2 x}{\partial x_0^s\, \partial v_0^r}(i,j,0) = 0, \quad r,s = 0,1,2, \quad r+s = 2,$$

$$c(i,j,0) = 0, \quad d(i,j,0) = 0.$$

Values of $g^{l,0}_{i,j}$ are given from (1) if $l = 0$ or from (4) if $l > 0$. The i,jth charge is

$$q^{l,0}_{i,j} = g^{l,0}_{i,j} \frac{c}{(1-u_j^2)^{3/2}} \Delta x_0 \Delta u.$$

(3) For a given time $\tau_l = lT_l$, $l = 0, 1, \ldots, M-1$:

For t_n, $n = 0, 1, 2, \ldots, N_g - 1$ we assume values for $g^{l,n}_{i,j}$, $x(i,j,t_n)$, $v(i,j,t_n)$, $\frac{\partial x}{\partial x_0}(i,j,t_n)$, $\frac{\partial v}{\partial x_0}(i,j,t_n)$, $\frac{\partial x}{\partial v_0}(i,j,t_n)$, $\frac{\partial v}{\partial v_0}(i,j,t_n)$, $a(i,j,t_n)$, $b(i,j,t_n)$, $\frac{\partial^2 x}{\partial x_0^s\, \partial v_0^r}(i,j,t_n)$, $\frac{\partial^2 x}{\partial x_0^s\, \partial v_0^r}(i,j,t_n)$, $c(i,j,t_n)$, $d(i,j,t_n)$, and $q^{l,n}_{i,j}$. The solution to the Poisson equation is approximated by the method of Section 2.2.6. The computations in the paper are done with $N_p = N_x$. The electric field, $\overline{E}(x(i,j,t_n),t_n)$, and derivatives $\frac{\partial \overline{E}}{\partial x}(x(i,j,t_n),t_n)$, $\frac{\partial^2 \overline{E}}{\partial x^2}(x(i,j,t_n),t_n)$ are computed at particle positions from (2.27)–(2.29). The solution values of ese($\bar{t}_k$), ke($\bar{t}_k$), and FE($\bar{t}_k$) are computed as in Section 2.4 with $k = lN_g + n$, $\bar{t}_k = lT_1 + t_n$.

Then at time t_{n+1}

(i) $\bar{g}^{n+1}_{i,j}$ is computed from (2.3), $\lambda = (\sum_{i,j} \bar{g}^{n+1}_{i,j} \frac{c}{(1-u_j^2)^{3/2}} \Delta x_0 \Delta u)/(\epsilon \sum_k h(x_k))$, and $g^{l,n+1}_{i,j} = \bar{g}^{n+1}_{i,j}/\lambda$.

(ii) $x(i,j,t_{n+1})$, $v(i,j,t_{n+1})$ are computed from (2.18) and (2.19).

(iii) $\frac{\partial x}{\partial x_0}(i,j,t_{n+1})$, $\frac{\partial v}{\partial x_0}(i,j,t_{n+l})$, $\frac{\partial x}{\partial v_0}(i,j,t_{n+1})$, $\frac{\partial v}{\partial v_0}(i,j,t_{n+1})$ are computed from (2.20)–(2.23),

$$a(i,j,t_{n+1}) = \exp(\beta t_{n+1}) \frac{\partial x}{\partial v_0}(i,j,t_{n+1}), \quad b(i,j,t_{n+1}) = \exp(\beta t_{n+1}) \frac{\partial x}{\partial x_0}(i,j,t_{n+1}).$$

(iv) $\frac{\partial^2 x}{\partial x_0^s\, \partial v_0^r}(i,j,t_{n+1})$, $\frac{\partial^2 v}{\partial x_0^s\, \partial v_0^r}(i,j,t_{n+1})$, are computed from (2.24) and (2.25),

$$c(i,j,t_{n+1}) = \mathrm{e}^{3\beta t_{n+1}} \left(\frac{\partial v}{\partial v_0} P_1 - \frac{\partial x}{\partial v_0} P_2\right)(i,j,t_{n+1}),$$

$$d(i,j,t_{n+1}) = \mathrm{e}^{3\beta t_{n+1}} \left(\frac{\partial x}{\partial x_0} P_2 - \frac{\partial v}{\partial x_0} P_1\right)(i,j,t_{n+1}),$$

where

$$P_1 = \left[-\frac{\partial^2 x}{\partial x_0^2}\left(\frac{\partial x}{\partial v_0}\right)^2 + 2\frac{\partial^2 x}{\partial x_0\,\partial v_0}\left(\frac{\partial x}{\partial v_0}\right)\left(\frac{\partial x}{\partial x_0}\right) - \frac{\partial^2 x}{\partial v_0^2}\left(\frac{\partial x}{\partial x_0}\right)^2 \right](i,j,t_{n+1}),$$

$$P_2 = \left[-\frac{\partial^2 v}{\partial x_0^2}\left(\frac{\partial x}{\partial v_0}\right)^2 + 2\frac{\partial^2 v}{\partial x_0\,\partial v_0}\left(\frac{\partial x}{\partial v_0}\right)\left(\frac{\partial x}{\partial x_0}\right) - \frac{\partial^2 v}{\partial v_0^2}\left(\frac{\partial x}{\partial x_0}\right)^2 \right](i,j,t_{n+1}).$$

(v) The charge at the i,jth trajectory is $q_{i,j}^{l,n+1} = g_{i,j}^{l,n+1}\frac{c}{(1-u_j^2)^{3/2}}\Delta u \Delta x_0$.

(4) For $n = N_g,\ t_{N_g} = T_1$:

For given $l = 0, 1, \ldots, M-1$ then $\bar{t}_k = lT_1 + t_{N_g} = (l+1)T_1 = \tau_{l+l}$ with $k = (l+1)N_g$. The solution along particle trajectories computed in (3) is reconstructed on the fixed grid on Ω as described in Section 2.3. This gives the initial function $g_{i,j}^{l+1,0}$ for Eq. (2.3) at time τ_{l+1}. If $l+1 < M$ then the computation returns to (2), and the cycle from (2) to (4) is repeated to compute the solution to (1.1) and (1.2) for $\bar{t}_k \in [(l+1)T_1, (l+2)T_1]$. If $l+1 = M$ then $k = MN_g = N_t$ and $g_{i,j}^{l+1,0} = g_{i,j}^{M,0}$ provides the approximate solution to (1.1) and (1.2) at $\bar{t}_{N_t} = T$. The ese, ke, and FE are computed at time T based on the function $g_{i,j}^{M,0}$, and the computational cycle is ended.

3. Computational examples

3.1. Steady state solution

For the time independent Vlasov–Poisson–Fokker–Planck system one can obtain an exact solution. This solution can be used as an initial distribution function for the time dependent problem. The resulting computation serves as a check on the accuracy of the numerical method.

We consider the set of equations

$$v\frac{\partial f}{\partial x} + E(x)\frac{\partial f}{\partial v} = q\frac{\partial^2 f}{\partial v^2} + \beta\frac{\partial}{\partial v}(vf), \quad 0 \leqslant x \leqslant 1, \quad -\infty < v < \infty,$$

$$E(x) = \frac{\partial \phi}{\partial x},$$

and $\phi(x)$ the solution to

$$\frac{\partial^2 \phi}{\partial x^2} = \int_{-\infty}^{\infty} f(x,v)\mathrm{d}v - h(x),$$

$$\phi(0) = \phi(1) = 0.$$

A solution is

$$f(x,v) = \exp\left(\cos(2\pi x) - \frac{\beta v^2}{2q}\right), \quad E(x) = -\frac{q}{\beta}(2\pi)\sin(2\pi x),$$
$$h(x) = \frac{q}{\beta}(2\pi)^2\cos(2\pi x) + \sqrt{\frac{2q\pi}{\beta}}\exp(\cos(2\pi x)). \tag{3.1}$$

The solution to the time dependent problem (1.1) and (1.2) is therefore computed by the method of Section 2 with initial function

$$f_0(x,v) = \exp\left(\cos(2\pi x) - \frac{\beta v^2}{2q}\right)$$

and the background charge distribution $h(x)$ given by (3.1).

Our goal is to estimate computationally the order of accuracy of the numerical method of Section 2. As a representative quantity for the solution we graph the electrostatic energy as a function of time which is given by expression (2.34). The discretized electrostatic energy, $\mathrm{ese}(\bar{t}_k)$, is computed according to (2.39). Fig. 1 gives the graph of $\mathrm{ese}(\bar{t}_k)$ for $0 \leqslant \bar{t}_k \leqslant 2$. Here $\beta = 0.1$, $q = 0.1$, $N_x \times N_v = 100 \times 100$, $\Delta t = 0.0001$ and $N_g = 4000$. Eq. (1.21) is approximated using the SOR method iterated to a tolerance of 10^{-11} as mentioned in Section 2.2.2. As expected for the steady state problem the graph is close to constant except, however, at points of regriding where discontinuities are apparent. The parameter, c, of (2.2) determines the range of discrete velocities used in the computation. This parameter can be adjusted to improve the quality of the computed solution. In the present computation we let $c = 2$. In subsequent computations this constant is a given different value.

Our first step is to see what effect the time parameter, Δt, has on the computation. Keeping the other parameters the same as for Fig. 1 the parameter Δt is varied as $\Delta t = 0.01, 0.001, 0.0001$. Fig. 2 shows the graph of ke for these values of Δt. It can be noted that the ke graphs computed from expression (2.37) are continuous at the regriding points. The dotted line shows the "exact" value of ke which was obtained by approximating the integral (2.35) using the function, $f(x,v)$, of (3.1) and $N_x \times N_v = 300 \times 300 = 90{,}000$ data points. We observe that the error in the computed solution for $t > 0$ decreases

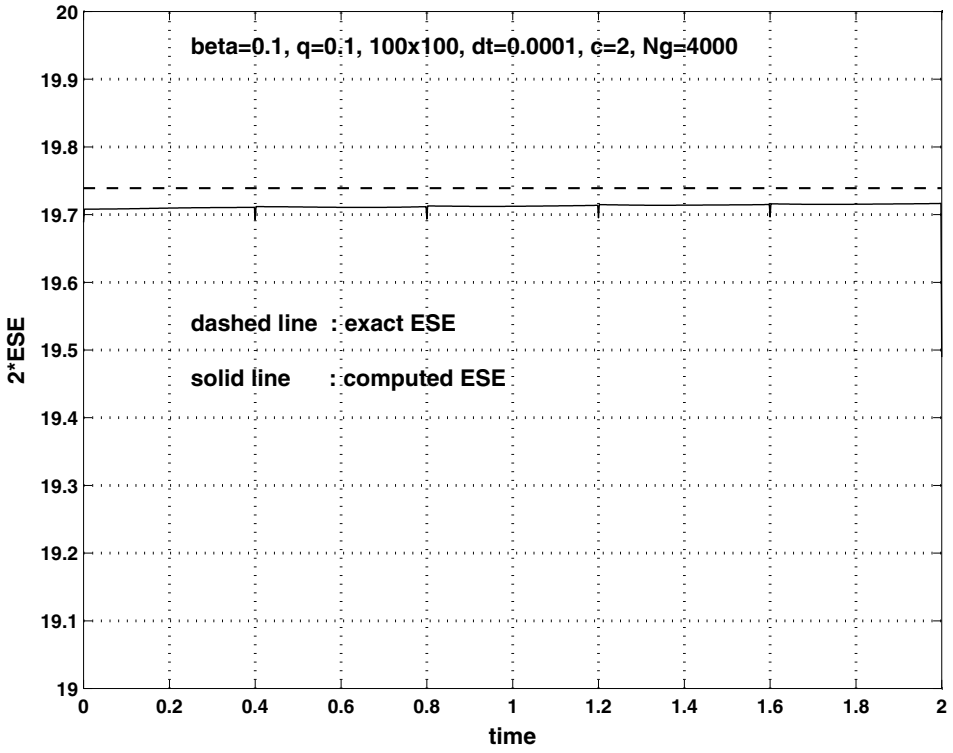

Fig. 1.

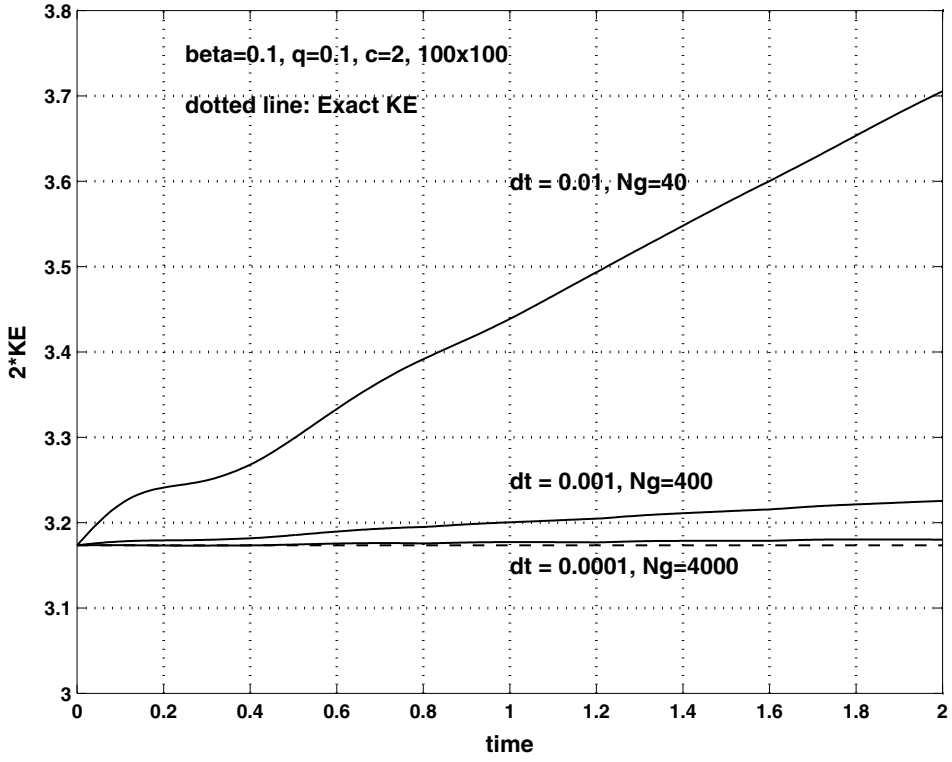

Fig. 2.

markedly with Δt and that the most accurate solution over the time interval [0,2] is with $\Delta t = 0.0001$, i.e., $\Delta t = O((\Delta x_0)^2 + (\Delta u)^2)$.

We make a further determination of the order of accuracy of the numerical method by computing the error in the electric field. Let x_k, $k = 1, \ldots, N_p - 1$ be the points on the Poisson mesh. Then $E(x_k) = -\frac{q}{\beta}(2\pi)\sin(2\pi x_k)$ is the exact value of the electric field, and $E_k(t)$ is the approximate field at the Poisson mesh points at time t. Let

$$e_2(t) = \frac{\sqrt{\sum_{k=1}^{N_p-1} (E(x_k) - E_k(t))^2}}{\sqrt{\sum_{k=1}^{N_p-1} E(x_k)^2}},$$

the relative l_2 error in the electric field. Fig. 3 shows the graphs of $e_2(t)$ for $N_x \times N_v \times \Delta t = 50 \times 50 \times 0.0004$, $70 \times 70 \times 0.0002$, $100 \times 100 \times 0.0001$. That is we use respectively 2500, 4900, 10,000 data points so that the number of data points is approximately doubled from one computation to the next, and the time step is halved. Also, $\Delta t = O((\Delta x_0)^2 + (\Delta u)^2)$ for these computations. Values of $e_2(t)$ are given in Table 1 for $t = 0$, 0.3, 1. We see that increasing the number of data points by a factor of two and reducing the time step by 1/2 approximately reduces the error by 1/2. This suggests that the error is $O(1/N + \Delta t)$ where N is the number of data points. But $(\Delta x_0)^2 + (\Delta u)^2 = C/N$, C a constant. Thus the computations indicate that the method has accuracy that is $O((\Delta x_0)^2 + (\Delta u)^2 + \Delta t)$. It can be noted that it is shown computationally in [18] that the particle-in-cell method for the Vlasov–Poisson system using a finite difference method to solve

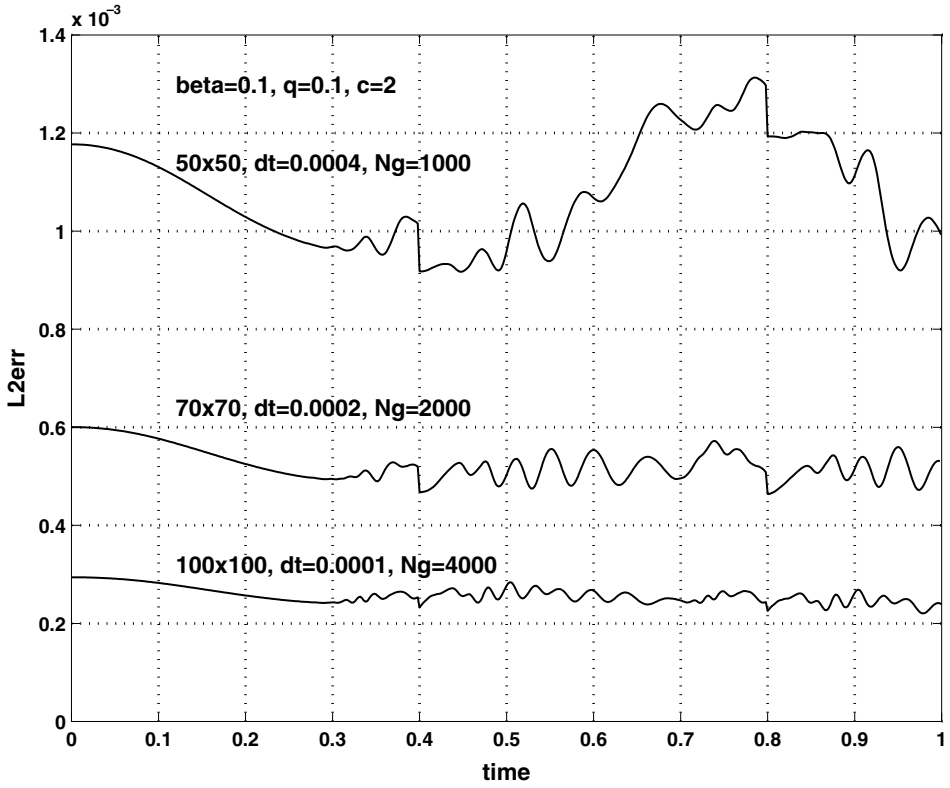

Fig. 3.

the Poisson equation is second order accurate in the spatial parameters assuming $N_p = N_x$. The method in [18] can only be $O(\Delta t)$ in the time parameter. Thus the order of accuracy presently obtained for nonzero q, β is consistent with this previous result for $q = \beta = 0$.

3.2. Time dependent solution, approach to steady state

It is known that the solution to the Vlasov–Poisson–Fokker–Planck system converges to a time independent steady state solution as $t \to \infty$ [3]. We demonstrate this property computationally by considering an initial distribution function of the form

$$f_0(x,v) = \frac{K}{\sqrt{2\pi}v_{\text{th}}}\left(1 + 2\epsilon\cos\left(\frac{2\pi x}{L}\right)\right)\exp\left(\frac{-v^2}{2v_{\text{th}}^2}\right), \quad 0 \leqslant x \leqslant L, \tag{3.2}$$

v_{th}, ϵ, L, K – constants and $h(x) = K$ in (1.3). If $\beta = q = 0$ then (1.1) and (1.2) becomes the Vlasov–Poisson system, and the solution with initial function (3.2) and $h(x) = K$ represents classical Landau damping. The Landau damping phenomenon is a characteristic of collisionless plasma that results in a damping of the plasma wave without energy dissipation through collisions with the surrounding medium. The physical mechanism that causes this is a transfer of energy from the wave to plasma particles that are moving with a velocity close to the phase velocity of the wave. However, if β, $q \neq 0$ then as time increases the dominant process becomes a dissipation of field energy as a result of the diffusion in velocity space. The solution,

Table 1
Relative l_2 error in the electric field

$N_x \times N_v \times \Delta t$	$e_2(t)$, $t = 0$	$e_2(t)$, $t = 0.3$	$e_2(t)$, $t = 1$
$50 \times 50 \times 0.0004$	11.32 D-4	9.683 D-4	9.907 D-4
$70 \times 70 \times 0.0002$	5.772 D-4	4.945 D-4	5.289 D-4
$100 \times 100 \times 0.0001$	2.828 D-4	2.429 D-4	2.389 D-4

$f(x,v,t)$, of (1.1) and (1.2) approaches a steady state as $t \to \infty$. It can be determined that the steady state solution is

$$f(x,v) = \frac{K}{\sqrt{2\pi q/\beta}} \exp\left(\frac{-v^2}{2q/\beta}\right). \tag{3.3}$$

When q, $\beta \neq 0$ the approach to steady state can be observed several ways. First, we can consider the electrostatic energy given by (2.34). At the steady state with $f(x,v,t)$ replaced by the function (3.3) and $h(x) = K$ in (1.3) it follows that $\rho(x) = 0$, $\phi(x) = 0$, and $E(x) = 0$. Thus for the solution to (1.1) and (1.2) with initial function (3.2) as $t \to \infty$ then ese $\to 0$. Secondly, the kinetic energy is given by (2.35). Replacing $f(x,v,t)$ in (2.35) by the function (3.3) and evaluating the integral it follows that as $t \to \infty$, 2ke $\to KLq/\beta$. Finally, a useful quantity for describing the convergence to steady state is the free energy defined by (2.36). It is shown in [3] that the free energy is a monotonically decreasing function of time that is bounded from below. Hence FE approaches a limit as $t \to \infty$. The proof in [3] is for an initial value problem in three dimensions. However, we can show computationally the applica-

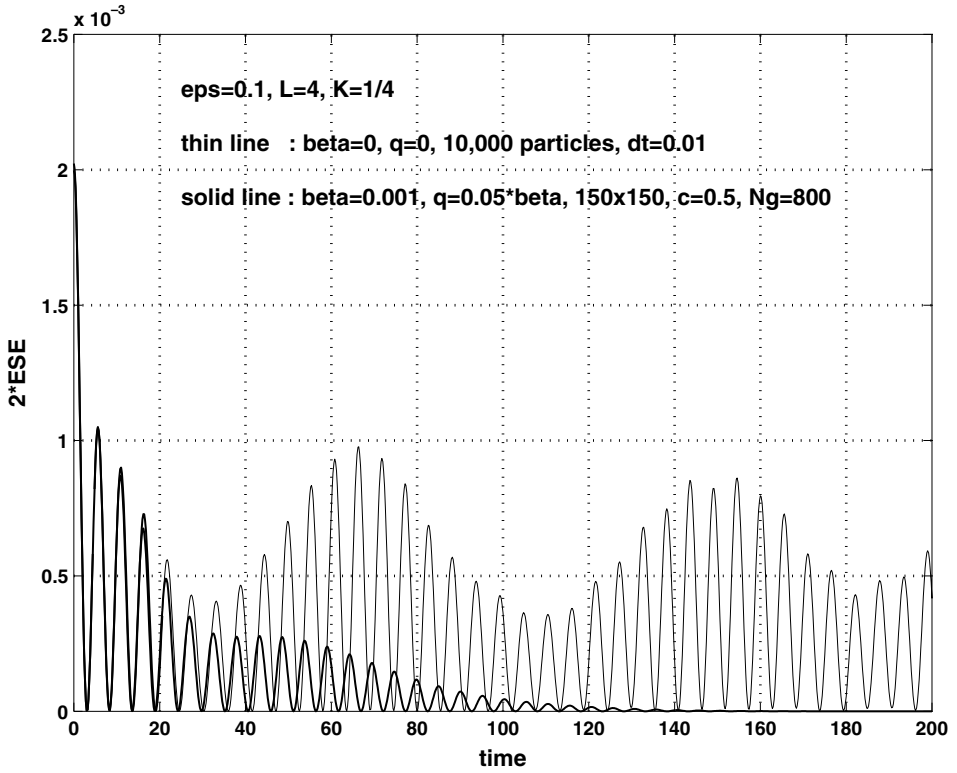

Fig. 4.

bility of this result to the present 1-D periodic problem. For the function (3.3) the entropy integral in (2.36) can be evaluated exactly. Along with the steady state values for 'ese' and 'ke' it can be determined that FE $\rightarrow \frac{KLq}{\beta}\ln(K/\sqrt{2\pi q/\beta})$ as $t \rightarrow \infty$.

To demonstrate the time asymptotic behavior we compute the solution to (1.1) and (1.2) with initial function (3.2) for varying q and β. In (3.2) let $\epsilon = 0.1$, $L = 4$, $v_{\text{th}} = 0.3/\pi$, $K = 1/4$. The thin line in Fig. 4 gives the graph of electrostatic energy for the case $q = \beta = 0$. That is this is the solution to the Vlasov–Poisson system with no Fokker–Planck diffusion. This computation was done with a particle-in-cell method similar to that in [18] using 10,000 initial data points. The slow non-monotonic decrease in the amplitude of oscillations in the graph of ese is indicative of a mild Landau damping.

To observe the convergence to steady state for q, $\beta \neq 0$ we now let β take on the values $\beta = 0.01, 0.0025, 0.001$, $q = 0.05\beta$ and compute the solution using the method of Section 2. For these computations $N_x \times N_v = 150 \times 150 = 22{,}500$ particles, $\Delta t = 0.01$. For $\beta = 0.001$ then $N_g = 800$. That is regriding is at time intervals $\Delta\tau = 8$. For $\beta = 0.0025, 0.01$, $N_g = 400$. Regriding is at intervals $\Delta\tau = 4$. The parameter, c, of (2.2) has the value $c = 0.5$. The iterative procedure (SOR) is used throughout to approximate (1.21). Since $q/\beta = 0.05$ in each case the solutions to (1.1) and (1.2) all converge to the same steady state solution as $t \rightarrow \infty$. The difference is in how fast the solutions converge to the limit. The solid line in Fig. 4 shows the graph of ese for $\beta = 0.001$, $q = 0.05\beta$ in comparison to the graph for q, $\beta = 0$. Fig. 5 gives the ese graphs for $\beta = 0.0025, 0.01$. As expected ese $\rightarrow 0$ as t gets large with the limit approached more rapidly for the larger q, β. For $q/\beta = 0.05$ the limiting value of ke for the given parameters is 2ke $\rightarrow KLq/\beta = 0.05$. Fig. 6 shows the graphs of kinetic energy for the three cases considered. The approach to the steady state value

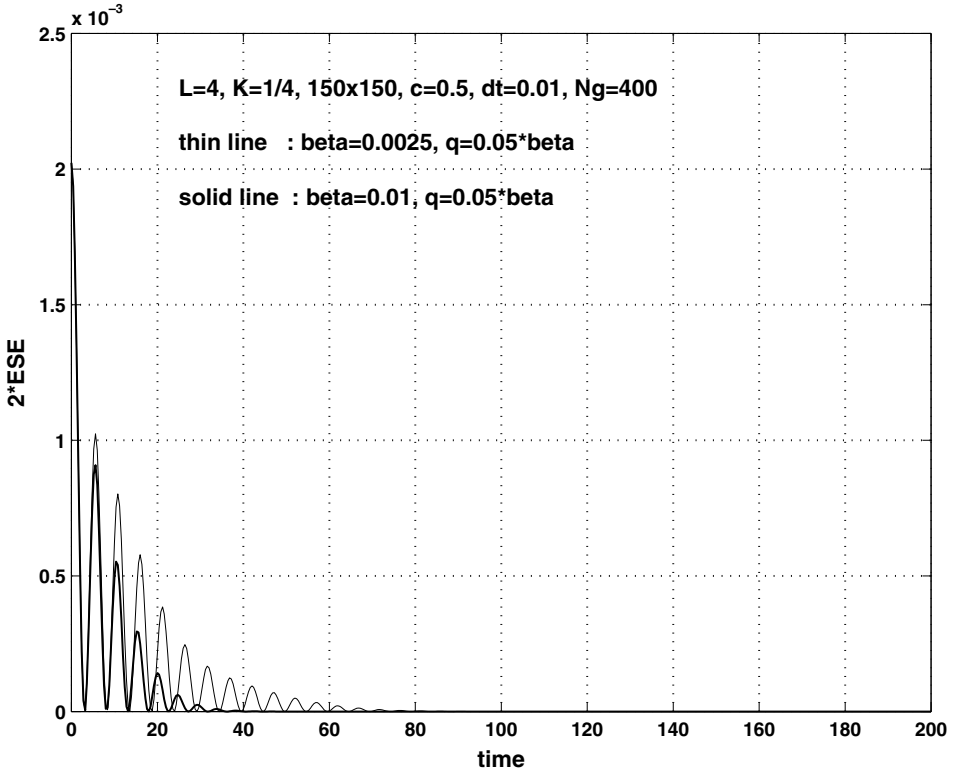

Fig. 5.

is reasonably clear. Fig. 7 shows the graphs of FE as a function of time for the three cases. The graphs are monotonically decreasing as expected based on the theory in [3] and approach a limiting greatest lower bound. For $K = 1/4$, $L = 4$, $q/\beta = 0.05$ then $\lim_{t\to\infty} \mathrm{FE} = \frac{KLq}{\beta} \ln(K/\sqrt{2\pi q/\beta}) \approx -0.04036834$. The graphs of FE in Fig. 7 show a good agreement with this theoretically determined limit. For a more quantitative measure we refer to Table 2. Here the computed FE is given at the end of the respective time intervals for $\beta = 0.001$, 0.0025, 0.01 and $q = 0.05\beta$.

As another example the solution to (1.1) and (1.2) is computed with some different constants in (3.2). We now let $\epsilon = 0.01$, $L = 1$, $v_{\mathrm{th}} = 0.3/\pi$, $K = 3.5$. The thin line in Fig. 8 gives the ese graph for the Vlasov–Poisson solution, i.e., $\beta = q = 0$. For this computation we use a particle-in-cell method. For the present set of parameters the graph of ese has a higher frequency of oscillation than the previous example and is somewhat more difficult to resolve computationally with the particle-in-cell method. Thus for the $q, \beta = 0$ case we use 40,000 data points. To observe the approach to steady state for $\beta, q \neq 0$ we let $\beta = 0.01$ and vary q as $q = 0.0001$, 0.00015, 0.0002. Now the ratio q/β varies, and the time dependent solutions approach different

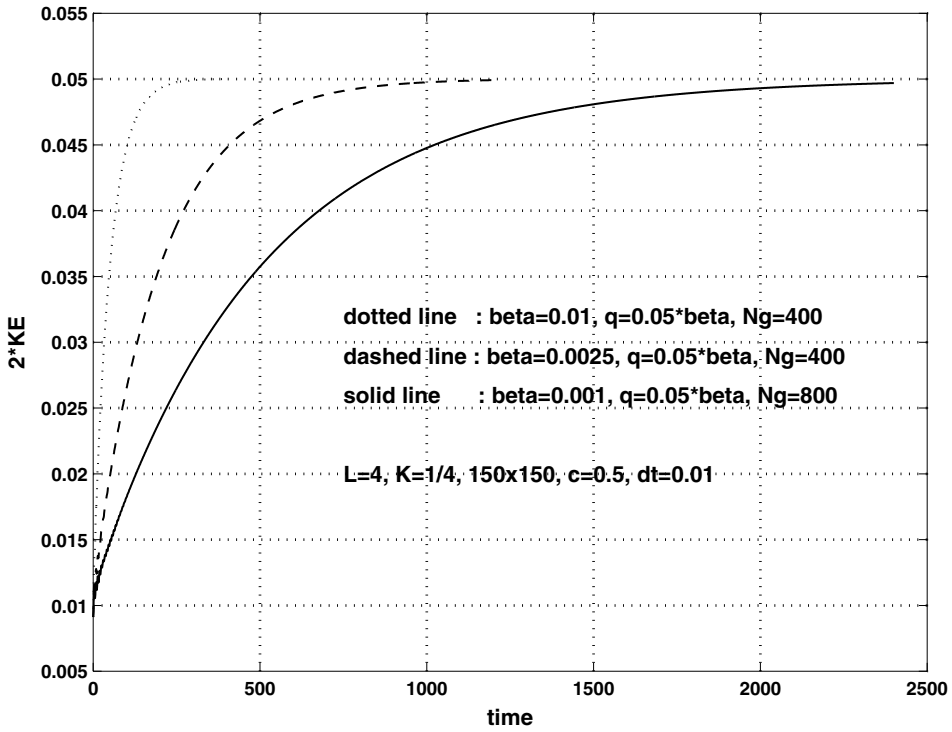

Fig. 6.

Table 2
Computed FE at time T, $q = 0.05\beta$

β	T	FE
0.001	2400	−0.04036779
0.0025	1200	−0.04036822
0.01	400	−0.04036827

Exact steady state FE ≈ -0.04036834.

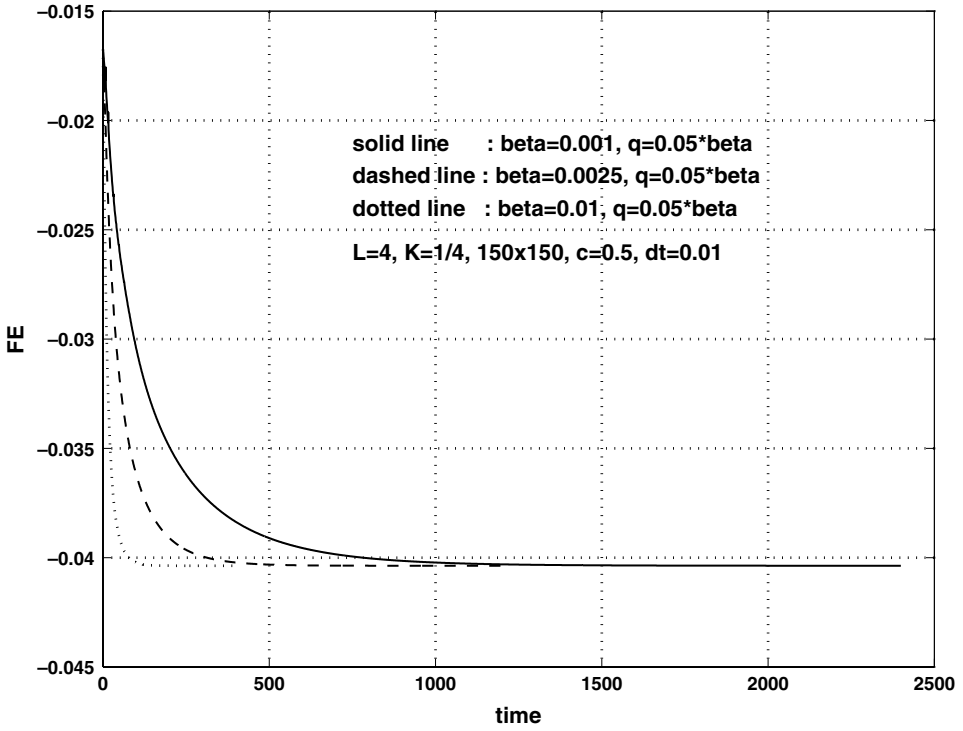

Fig. 7.

steady state solutions. The computations are done by the method of Section 2 with $N_x \times N_v = 100 \times 100 = 10{,}000$ particles, $\Delta t = 0.01$, $N_g = 400$. Thus regriding is at intervals $\Delta\tau = 4$. For the constant in (2.2) $c = 0.5$. It can be noted that the method of Section 2 which includes the regriding requires fewer initial data points for a stable computation than the particle-in-cell method which does not include regriding used for β, $q = 0$. In all cases the graphs of ese approach zero; however, the convergence to the limit is more rapid for the larger value of q. The graph of ese for $\beta = 0.01$, $q = 0.0001$ is in Fig. 8 in comparison to the graph for $\beta = q = 0$. The ese graphs for $\beta = 0.01$, $q = 0.00015$ and $\beta = 0.01$, $q = 0.0002$ are in Fig. 9. The difference in the steady state solutions is seen clearly in the graphs of the kinetic energy. For $q = 0.0001$, $2\text{ke} \to KLq/\beta = 0.035$, for $q = 0.00015$, $2\text{ke} \to 0.0525$, and for $q = 0.0002$, $2\text{ke} \to 0.07$. This is demonstrated clearly in Fig. 10. The free energy graphs decrease monotonically, but in this case approach different limits. The FE graph for $\beta = 0.01$, $q = 0.0002$ is shown in Fig. 11. For $K = 3.5$, $L = 1$, $q/\beta = 0.02$ then $\lim_{t\to\infty}\text{FE} = \frac{KLq}{\beta}\ln(K/\sqrt{2\pi q/\beta}) \approx 0.16028852$. The graph of Fig. 11 is in agreement with this limiting value of FE. By comparison to the exact steady state value of FE the computed value in Fig. 11 at $T = 400$ is FE = 0.16028863.

We comment briefly on the choice of the regrid parameters, T_1, N_g, where $T_1 = N_g\Delta t = \Delta\tau$, the regrid interval. As t_n increases on the interval $[0,T_1]$, $t_n = n\Delta t$, $n = 0,\ldots,N_g$, the coefficients $a(i,j,t_n)$, $b(i,j,t_n)$ in (2.3) increase, and the quantity $\Theta(t_n)$, defined in Section 2.2.2, also increases. The closer $\Theta(t_n)$ gets to one the more iterations are required for convergence of the SOR method. Thus N_g and T_1 are chosen sufficiently small so as to limit the number of iterations required for the SOR algorithm. Reducing T_1 can also improve the long term stability and accuracy of the method and keep discontinuities at the regriding step from becoming too pronounced. However, N_g and T_1 are chosen sufficiently large so that most of the computation goes into the particle cycle of Section 2.2 and not

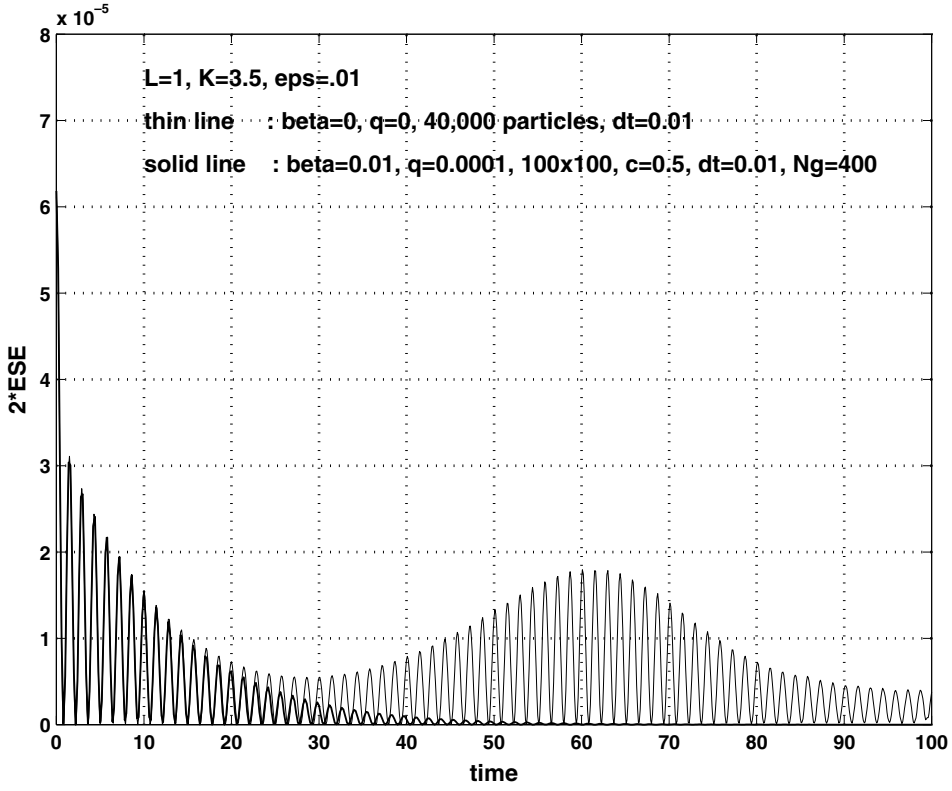

Fig. 8.

into the regriding step of Section 2.3. Also, the smaller q, the faster the convergence of the SOR method, and the larger one may be able to take N_g and T_1. So, for example, in the computation given by the solid line in Figs. 9 and 10, $q = 0.0002$, $\Delta t = 0.01$, $N_g = 400$, $T_1 = 4$, at the beginning of a particle cycle the SOR method converges to a tolerance of 10^{-11} with about 7 iterations and at the end of the particle cycle the convergence requires about 14 iterations. For this example there is very little change in the computed solution if instead of using $N_g = 400$, $T_1 = 4$ we let $N_g = 200$, $T_1 = 2$. Thus, within limits the regrid parameters need not be specified very precisely. For the computation given by the solid line in Figs. 4 and 6, $q = 0.00005$, $\Delta t = 0.01$, $N_g = 800$, $T_1 = 8$, the SOR method converges to a tolerance of 10^{-8} with 4–5 iterations on the entire particle cycle. We note that the tolerance for the SOR method is 10^{-8} for the computations of Figs. 4–7. For all other computations it is 10^{-11}. We do not have a specific formula for setting the regrid parameters. For a given initial data and parameters, q, β, some experimentation over a few computational cycles was required to determine suitable values for T_1, N_g.

4. Some other numerical methods

In this section we consider some other ways of approximating the solution to (1.1) and (1.2). This allows us both to determine with more certainty the validity of our computations and also to point to possible

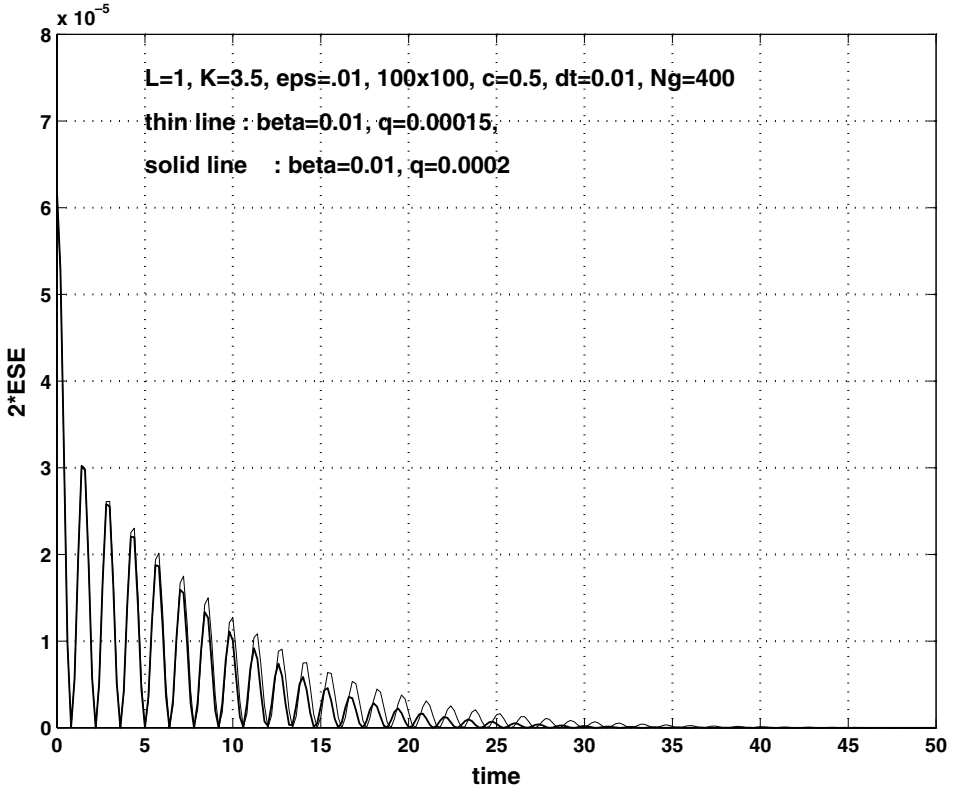

Fig. 9.

advantages the present numerical method may have over other methods. Two methods considered are the random particle method described in [1,9] and the finite difference method of [14].

We start with the random particle method. The method derives from the stochastic interpretation of the convection–diffusion process which is given in terms of the Langevin equation

$$\mathrm{d}x = v\,\mathrm{d}t, \tag{4.1}$$

$$\mathrm{d}v = (E(x,t) - \beta v)\mathrm{d}t + \sqrt{2q}\,\mathrm{d}B(t). \tag{4.2}$$

Here $B(t)$ represents Brownian motion. With some suitable assumptions the PDE (1.1) can be derived on the basis of Eqs. (4.1) and (4.2) as is done in [5]. The random particle method as applied to the Vlasov–Poisson–Fokker–Planck system numerically approximates the solutions to (4.1) and (4.2). Our application of this method to approximate the solution to (1.1) and (1.2) proceeds as follows: phase space is partitioned as in Section 2.1. That is,

$$x_{0_i} = \left(i - \frac{1}{2}\right)\Delta x_0, \quad i = 1, \ldots, N_x,$$

$$u_j = -1 + j\Delta u, \quad j = 1, \ldots, N_v,$$

$$v_{0_j} = \frac{cu_j}{\sqrt{1 - u_j^2}}. \tag{4.3}$$

This distribution of initial data points (x_{0_i}, v_{0_j}) is referred to as uniform (in x_0,u) in contrast to an asymptotic initial distribution to be considered subsequently. The partition in the time variable is $t_n = n\Delta t$, $n = 0, 1, \ldots, N_t$, $T = N_t\Delta t$ and $t_{n+1/2} = t_n + \Delta t/2$. approximate trajectories are defined as $x(i,j,t_n)$, $v(i,j,t_n)$ such that $x(i,j,0) = x_{0_i}$, $v(i,j,0) = v_{0_j}$. These trajectories satisfy a numerical approximation to the stochastic differential equations (4.1) and (4.2). The method we use is due to Chang [6], and which is also described in [1]. Following the description in [1] if $x(i,j,t_n)$, $v(i,j,t_n)$ are given then the values at time t_{n+1} are computed as

$$\begin{aligned}(1)\quad & x_{i,j}^{n+1/2} = x(i,j,t_n) + \frac{\Delta t}{2} v(i,j,t_n),\\ & v_{i,j}^{n+1/2} = v(i,j,t_n) + \frac{\Delta t}{2}\left(\overline{E}(x(i,j,t_n),t_n) - \beta v(i,j,t_n)\right),\end{aligned} \tag{4.4}$$

$$\begin{aligned}(2)\quad & x(i,j,t_{n+1}) = x(i,j,t_n) + \Delta t v_{i,j}^{n+\frac{1}{2}} + (\Delta t)^{\frac{3}{2}}\sqrt{2q}\left(\frac{1}{2}\phi_{n,1} + \frac{\sqrt{3}}{6}\phi_{n,2}\right),\\ & v(i,j,t_{n+1}) = v(i,j,t_n) + \frac{\Delta t}{2}\left(\overline{E}(x_{i,j}^{n+\frac{1}{2}}, t_{n+\frac{1}{2}}) - \beta v_{i,j}^{n+\frac{1}{2}}\right)\\ & \qquad - \beta(\Delta t)^{\frac{3}{2}}\sqrt{2q}\left(\frac{1}{2}\phi_{n,1} + \frac{\sqrt{3}}{6}\phi_{n,2}\right) + \sqrt{\Delta t(2q)}\phi_{n,1}.\end{aligned} \tag{4.5}$$

Here $\phi_{n,1}$ and $\phi_{n,2}$ are independent normally-distributed random numbers with zero mean and unit variance and $\overline{E}(x(i,j,t_n),t_n)$ is the approximate electric field.

To derive the self consistent field for the solution of (1.1) and (1.2) one associates with each trajectory a charge

$$q_{i,j} = \frac{c f_0(x_{0_i}, v_{0_i})\Delta u \Delta x_0}{\lambda(1-u_j^2)^{3/2}}, \tag{4.6}$$

where

$$\lambda = \left(\sum_{i,j} f_0(x_{0_i}, v_{0_i})\frac{c}{(1-u_j^2)^{3/2}}\Delta u \Delta x_0\right) \Big/ \left(\epsilon \sum_k h(x_k)\right).$$

The constant λ is computed in Section 2.2.1 and is needed to insure total charge neutrality. At time t_n the solution to (1.1) has an approximation of the form

$$\bar{f}(x,v,t_n) = \sum_{i,j} q_{i,j}\delta(x - x(i,j,t_n))\delta(v - v(i,j,t_n))$$

and the discrete charge density is given as

$$\tilde{\rho}(x,t_n) = \sum_{i,j} q_{i,j}\delta(x - x(i,j,t_n)) - h(x).$$

From the function $\tilde{\rho}(x,t_n)$ one computes the approximate field $\overline{E}(x,t_n)$ exactly as in Section 2.2.6. At the half step, time $t_{n+1/2}$, the field $\overline{E}$ is computed on the basis of a $\tilde{\rho}(x,t)$ in which $x(i,j,t_n)$ is replaced with $x_{i,j}^{n+1/2}$.

The random particle method is used to compute the solution to (1.1) and (1.2) for which the initial data, $f_0(x,v)$, is given by (3.2). The background charge in (1.3) is given by $h(x) = K$ as in Section 3.2. In (3.2) the various parameters are $\epsilon = 0.1$, $L = 4$, $v_{\text{th}} = 0.3/\pi$, $K = 1/4$. In (1.1), (4.4) and (4.5) we let $\beta = 0.001$, $q = 0.05\beta$. The constant in (4.3) is $c = 0.5$. We have previously computed the solution to (1.1) and (1.2) with this initial data and parameters q, β by the method of Section 2. We will refer to the method of Section 2 as the deterministic particle (DP) method. The ese graph computed by the deterministic particle method is gi-

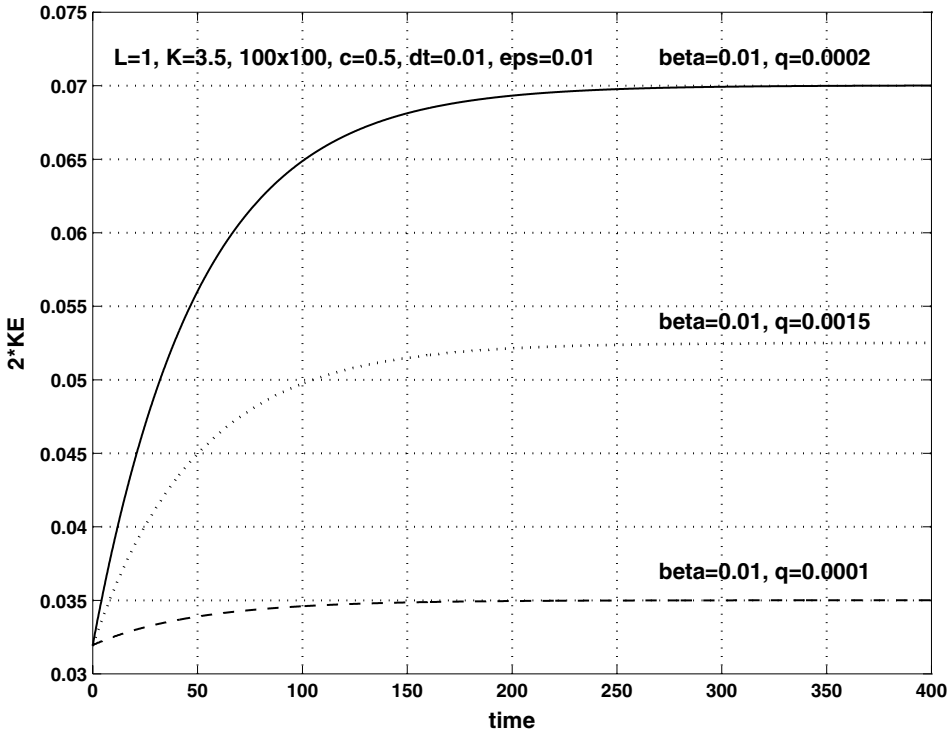

Fig. 10.

ven by the solid line in Fig. 4 and the ke graph is shown by the solid line in Fig. 6. We compute these same quantities using the random particle method. The ese is computed from the approximate field, $\overline{E}$, at the particle positions the same way as in Section 2.4. The ke is computed from the approximate trajectories given by (4.4) and (4.5) and the charge, $q_{i,j}$, (4.6), as

$$\text{ke} = \frac{1}{2}\sum_{i,j}(v(i,j,t_n))^2 q_{i,j}.$$

Fig. 12 gives the graph of ke and Fig. 13 the graph of ese for the random particle method in which particle trajectories are computed by (4.4) and (4.5). Here $N_x \times N_v = 200 \times 400 = 80{,}000$ particles and $\Delta t = 0.01$. For the Poisson mesh the parameter is $N_p = 200$. Increasing the number of discrete velocities improves the quality of the computed solution which is the reason for using more points in velocity space than in position space. The dotted line in Fig. 12 and the thin line in Fig. 13 represent the solution computed by the method of Section 2 (the DP method), that is the dotted line in Fig. 12 is the same graph as the solid line in Fig. 6 and the thin line in Fig. 13 is the same graph as the solid line in Fig. 4. These graphs demonstrate a very good agreement between the random particle method based on (4.3)–(4.5) and the method of Section 2.

A second example is now considered with a different set of parameters for $f_0(x,v)$ given by (3.2). We let $\epsilon = 0.01$, $L = 1$, $v_{\text{th}} = 0.3/\pi$, $K = 3.5$. The parameters β, q are $\beta = 0.01$, $q = 0.0002$. This example was previously computed by the deterministic particle method. The ese graph is the solid line in Fig. 9 and the ke graph is the solid line in Fig. 10. The random particle method based on (4.3)–(4.5) is therefore applied to compute the solution to (1.1) and (1.2) for this second set of parameters. As in the previous example

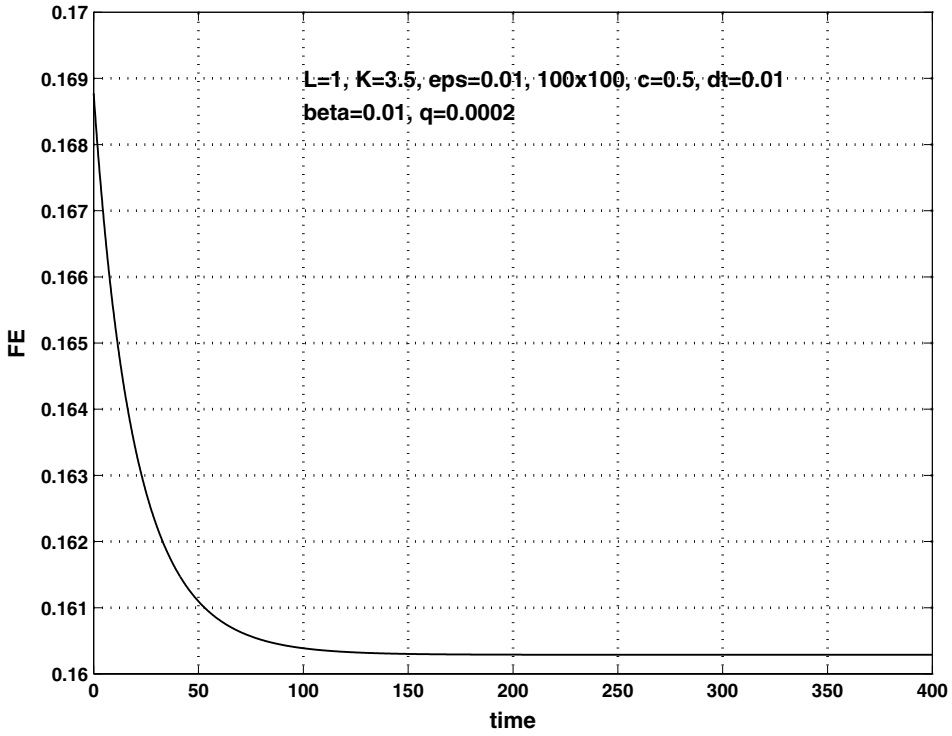

Fig. 11.

$N_x \times N_v = 200 \times 400 = 80{,}000$ particles, $\Delta t = 0.01$, $N_p = 200$. The solid line in Fig. 14 shows the graph of ke and the dashed line in Fig. 15 the graph of ese in comparison to the quantities previously computed by the deterministic particle method (the dotted line in Fig. 14 and the solid line in Fig. 15.) The ke graphs demonstrate a reasonably good correspondence between the two methods; however, from Fig. 15 it is seen that the ese graph is not well resolved by the random particle method. It can be noted that the electrostatic energy is a smaller quantity and has a more rapid oscillation for the present example than for the previous example. This may account for the increased difficulty in computing it accurately.

A question one might ask is whether the results obtained with the random particle method, in particular the ese graph in Fig. 15, can be improved with a different way of distributing the initial data points. To address this question we compute the solution to (1.1) and (1.2) using the random particle method with initial data asymptotically distributed according to a low discrepancy sequence of points. Initial distributions of this type have been used in applying particle methods to solve the Vlasov–Poisson system and are known to have good accuracy and stability properties. We use the low discrepancy sequence based on Fibonacci numbers applied by Neunzert and Wick in [12].

To compute with asymptotically distributed points we follow the procedure described in [19] where some similar computations are done for the Vlasov–Poisson system. For the initial distribution function for (1.1) and (1.2) let $f_0(x,v) = h(v)g(x)$ where

$$g(x) = 1 + 2\epsilon cos\left(\frac{2\pi x}{L}\right), \quad 0 \leqslant x \leqslant L \tag{4.7}$$

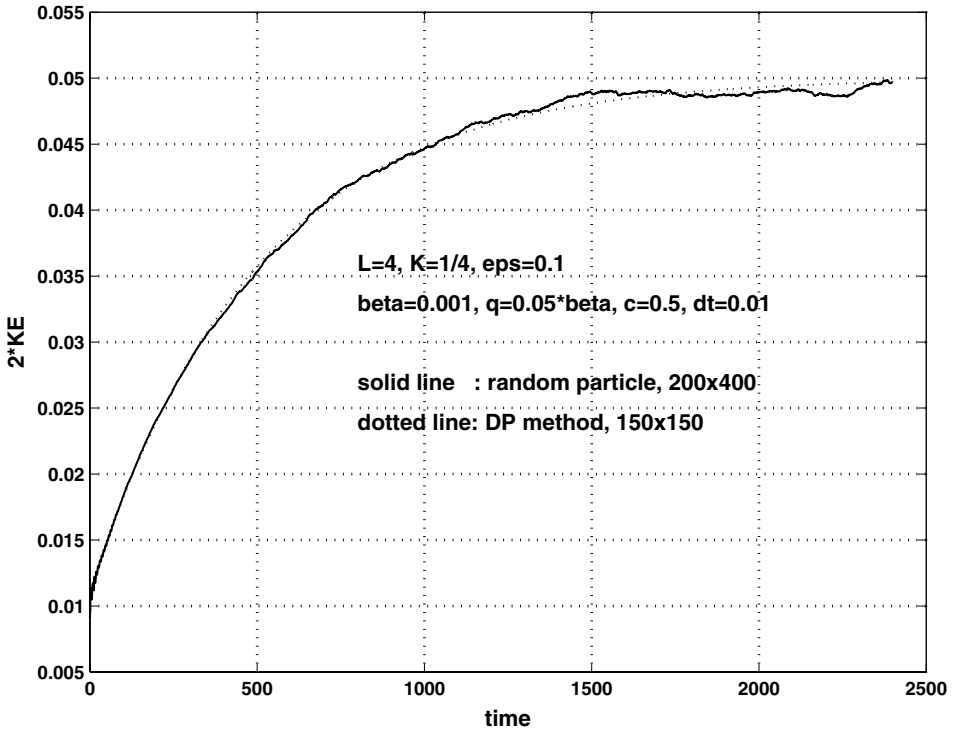

Fig. 12.

and

$$h(v) = \begin{cases} \frac{K}{C\sqrt{2\pi}v_{\text{th}}} \mathrm{e}^{-v^2/(2v_{\text{th}}^2)}, & v_{\min} \leqslant v \leqslant v_{\max}, \\ 0, & v < v_{\min} \text{ or } v > v_{\max}. \end{cases} \tag{4.8}$$

Here

$$C = \frac{1}{\sqrt{2\pi}v_{\text{th}}} \int_{v_{\min}}^{v_{\max}} \mathrm{e}^{-\frac{v^2}{2v_{\text{th}}^2}} \mathrm{d}v.$$

Thus

$$\int_0^1 \int_{-\infty}^{\infty} f_0(x,v)\mathrm{d}v\, \mathrm{d}x = KL.$$

To obtain the initial particle distribution in phase space we start with a sequence of points in the unit square as follows: let α_k be the k_{th} Fibonacci number, i.e., $\alpha_0 = \alpha_1 = 1$ and $\alpha_{k+1} = \alpha_k + \alpha_{k-1}$, and let $N = \alpha_k$. Then let

$$\begin{aligned} e_{1,i} &= \frac{2i-1}{2\alpha_k}, \\ e_{2,i} &= \left\{ \frac{2(i-1)\alpha_{k-1}+1}{2\alpha_k} \right\}, \quad i = 1, \ldots, N, \end{aligned} \tag{4.9}$$

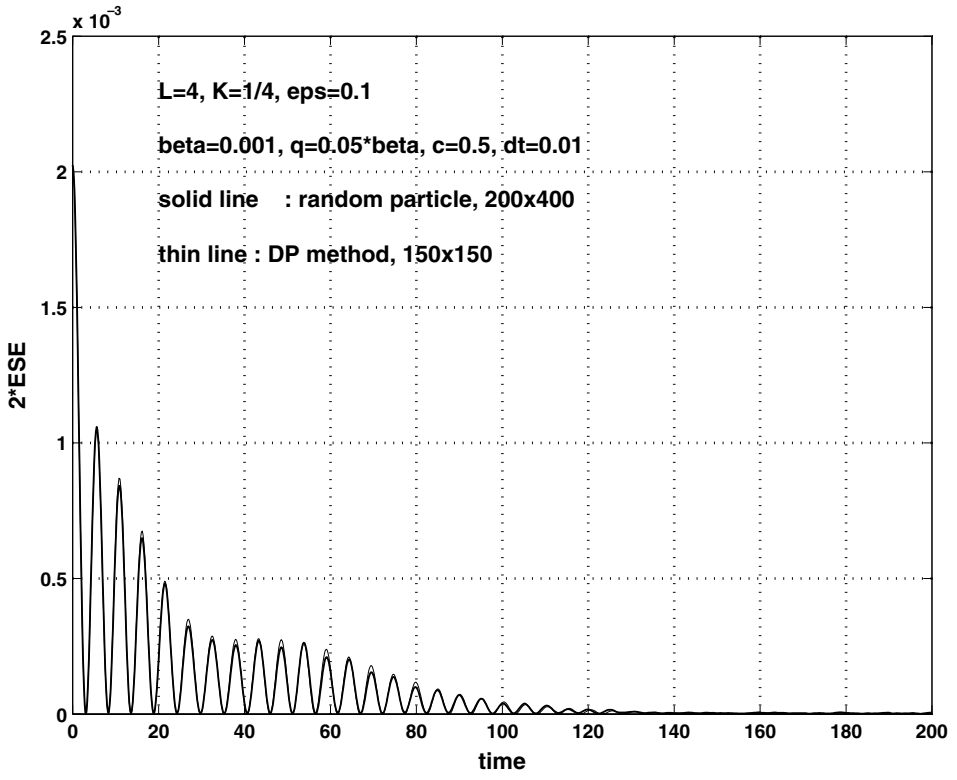

Fig. 13.

where $\{x\}$ refers to the fractional part of x. The points $(e_{1,i},e_{2,i})$ comprise a low discrepancy sequence of N points in the unit square. The coordinates of the initial data points in phase space are (x_{0_i}, v_{0_i}), $i = 1, \ldots, N$ which are obtained as solutions to the equations

$$e_{1,i} = \frac{1}{L}\int_0^{x_{0_i}} g(x)\mathrm{d}x, \qquad e_{2,i} = \frac{1}{K}\int_{v_{\min}}^{v_{0_i}} h(v)\mathrm{d}v.$$

Applying now the Chang method to approximate the stochastic differential equations (4.1) and (4.2) we let $x(i,0) = x_{0_i}$, $v(i,0) = v_{0_i}$, $i = 1, \ldots, N$. Then for $n = 0, 1, \ldots, N_t$ given $(x(i,t_n),v(i,t_n))$ the quantities $(x(i,t_{n+1}),v(i,t_{n+1}))$ are computed by expressions (4.4) and (4.5) in which the indices (i,j), $i = 1, \ldots, N_x$, $j = 1, \ldots, N_v$ are replaced by the single index $i = 1, \ldots, N$. Along each trajectory the charge $q_{i,j}$ given by (4.6) is replaced by $q_i = KL/N$. Thus the charge along each trajectory is a constant, and the total charge is $\sum_{i=1}^{N} q_i = KL$.

To compute the approximate electric field in (4.4) and (4.5) a discrete charge density is now defined as

$$\tilde{\rho}(x,t_n) = \sum_{i=1}^{N} q_i \delta(x - x(i,t_n)) - h(x) = \sum_{i=1}^{N} \frac{KL}{N}\delta(x - x(i,t_n)) - h(x).$$

With $\tilde{\rho}(x,t_n)$ so defined, and similarly at time $t_{n+1/2}$, the approximate field $\overline{E}(x,t_n)$, $\overline{E}(x,t_{n+1/2})$ is computed as in Section 2.2.6.

The random particle method with initial points asymptotically distributed is applied to compute the solution to (1.1) and (1.2) of Figs. 14 and 15. Thus in (4.7) and (4.8) the parameters ϵ, L, K, v_{th} are as pre-

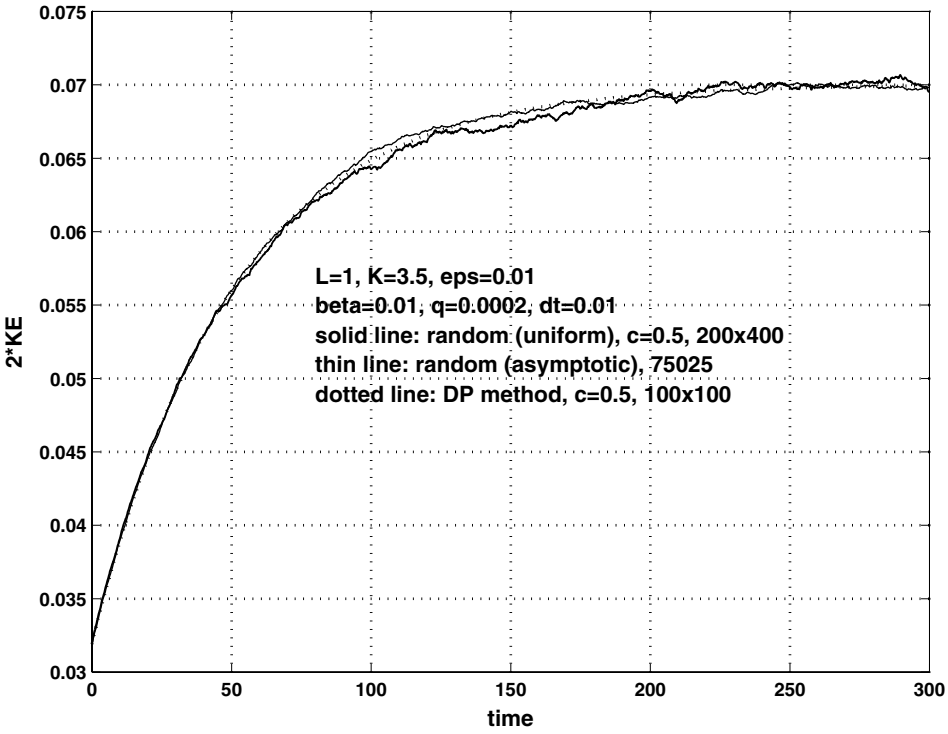

Fig. 14.

viously given for the solution with uniformly distributed initial points. In (4.8) we let $v_{\max} = 10v_{\text{th}}$, $v_{\min} = -10v_{\text{th}}$. The Fibonacci number α_k is taken as $\alpha_{24} = 75025$. Thus $N = 75025$ initial data points are used in the computation, $\Delta t = 0.01$, $N_p = 200$. The thin line in Fig. 14 is the ke graph and the thin line in Fig. 15 is the ese graph computed according to the random particle method with asymptotically distributed initial data. The quality of the solution computed with asymptotically distributed initial points is somewhat better than the solution based on initial points uniformly distributed in the x_0,u variables (shown by the solid line in Fig. 14 and the dashed line in Fig. 15). However, the problem of resolving accurately the graph of electrostatic energy still remains. We note that the random particle method with asymptotically distributed initial data was also applied to the problem of Figs. 12 and 13. A good agreement was obtained for this example between the asymptotic method and the other methods of approximation.

We also approximated Eqs. (4.1) and (4.2) using the 1.5 strong scheme referenced in [11, p. 383] and which is used for the numerical experiments in [15]. The random particle method with this different method for approximating the stochastic differential equations was applied to the two examples of Figs. 12–15. Here the initial data was given the uniform distribution in the x_0,u variables. The results were very similar to those we get with the Chang method. Thus we did not get an accurate representation for the ese graph of Fig. 15 using the random particle method. The graphs in Figs. 13 and 15 make it appear that the random particle method approximates the solution to (1.1) and (1.2) of Fig. 13 more accurately than the solution of Fig. 15. However, this is not necessarily the case. If one graphs the ese curve of Fig. 13 for small values on a fine scale what is observed is that the random particle method does not resolve accurately the electrostatic energy for values smaller than approximately 10^{-5}, and this is similarly the case for the graph of

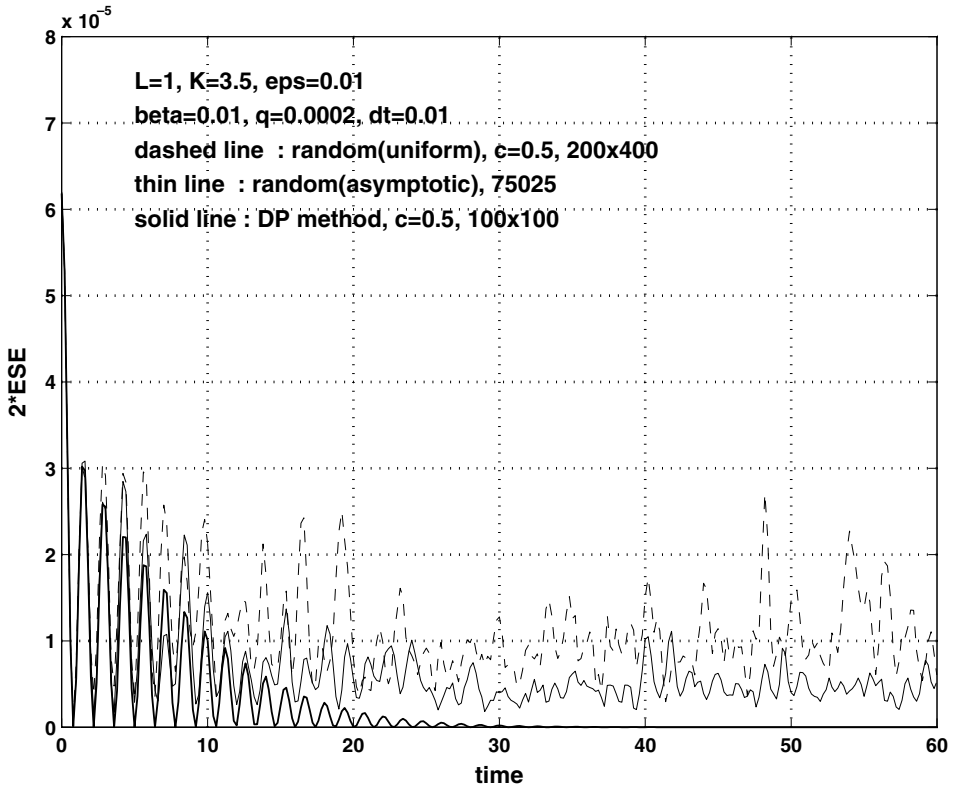

Fig. 15.

electrostatic energy of Fig. 15. What is also observed is that the deterministic particle method obtains a good resolution of the ese graph with well defined oscillations to very much smaller values than are resolved by the random particle method.

We now consider the finite difference method of [14]. Let Eq. (1.1) be written as

$$\frac{\partial f}{\partial t} + v\frac{\partial f}{\partial x} + E(x,t)\frac{\partial f}{\partial v} = \beta\frac{\partial}{\partial v}(vf) + q\frac{\partial^2 f}{\partial v^2}. \tag{4.10}$$

The left side of (4.10) is the Vlasov–Poisson part and the right side is the Fokker–Planck part of the equation. In [14] the approximation to the solution to (1.1) is maintained on a fixed rectangular grid in phase space. The Fokker–Planck part of the equation is approximated by a finite difference method on the fixed grid. The differencing in time is done along characteristic directions associated with the Vlasov–Poisson part of the equation. This requires that function values be interpolated from points on the grid to points off the grid at each step of the computation. The techniques used for the differencing in time are similar to those of Cheng and Knorr in [7]. For the detailed description of the numerical method we refer to [14].

The finite difference method is applied on a region of phase space $\mathscr{A} = \{(x,v)/0 \leqslant x \leqslant 1, -W \leqslant v \leqslant W\}$ for a positive number W. Let M_x, M_v, M_t be positive integers, $\Delta x = 1/M_x$, $\Delta v = W/M_v$. Then the region $\mathscr{A}$ is partitioned as $x_i = i\Delta x$, $i = 0, 1, \ldots, M_x$ and $v_j = j\Delta v$, $j = -M_v, \ldots, M_v$. The time interval $[0,T]$ is partitioned as $t_n = n\Delta t$, $n = 0,1, \ldots, M_t$, $T = M_t\Delta t$. If $f(x,v,t)$ is the solution to (1.1) and (1.2) then the approximation to $f(x_i,v_j,t_n)$ is denoted $f^n_{i,j}$. The electric field is computed at a half step in time, $t_{n+1/2} = t_n + \Delta t/2$, at

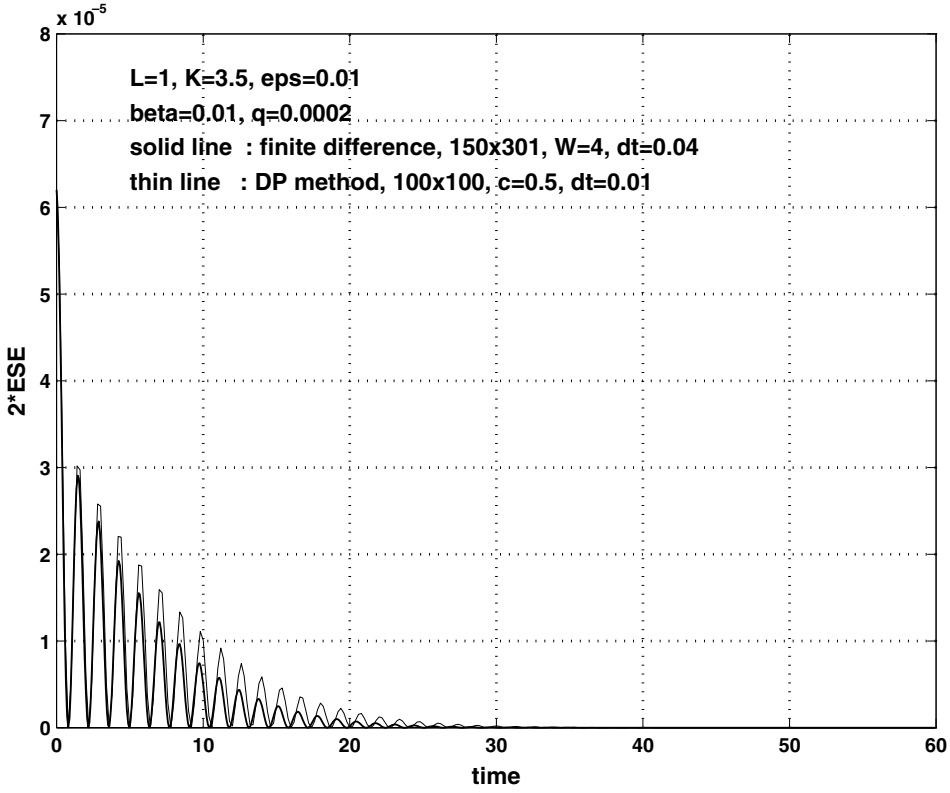

Fig. 16.

grid points x_i, $i = 0, 1, \ldots, M_x$ and is denoted $E_i^{n+1/2}$. Given the initial function to (1.1), $f_0(x,v)$, at time $t_n = 0$ then $f_{i,j}^0 = f_0(x_i, v_j),\ i = 0, 1, \ldots, M_x,\ j = -M_v, \ldots, M_v$. The subsequent values $f_{i,j}^n,\ E_i^{n+1/2},\ n > 0$ are computed by the method of [14]. To compare the method with that of Section 2 we compute the ese, ke, and FE. The ese is computed as

$$\mathrm{ese}(t_n) = \frac{1}{2}\sum_{i=0}^{M_x-1}\left(\frac{E_i^{n+1/2} + E_{i+1}^{n+1/2}}{2}\right)^2 \Delta x.$$

There is a small discrepancy here in that our value for ese at time t_n is based on field values computed at the half step. However, we determine that this discrepancy has a negligible effect. The ke and entropy, ent, are computed as

$$\mathrm{ke}(t_n) = \frac{1}{2}\sum_{i=0}^{M_x-1}\sum_{j=-M_v}^{M_v}(v_j)^2 f_{i,j}^n \Delta x \Delta v,$$

$$\mathrm{ent}(t_n) = -\sum_{i=0}^{M_x-1}\sum_{j=-M_v}^{M_v} f_{i,j}^n \ln(f_{i,j}^n)\Delta x \Delta v.$$

and $\mathrm{FE} = \mathrm{ese}(t_n) + \mathrm{ke}(t_n) - q/\beta\ \mathrm{ent}(t_n)$.

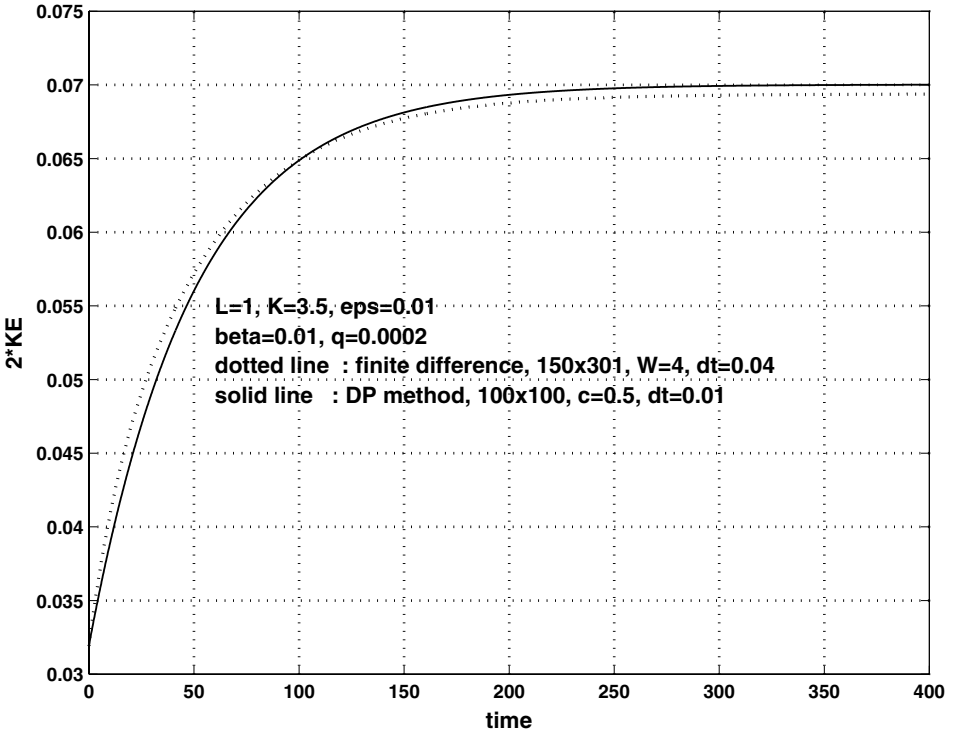

Fig. 17.

The finite difference method of [14] is applied to the example that was computed by the random particle method for Figs. 14 and 15. [1] That is, the initial data, $f_0(x,v)$, is given by (3.2) with parameters $\epsilon = 0.01$, $L = 1$, $v_{\text{th}} = 0.3/\pi$, $K = 3.5$, the background charge is $h(x) = K$, the parameters β, q are $\beta = 0.01$, $q = 0.0002$. Figs. 16–18 show the graphs of ese, ke, and FE computed by the finite difference method. The grid parameters for these computations are $W = 4$, $M_x, M_v = 150,150$, $\Delta t = 0.04$. The total number of data points on the grid is $M_x \times (2M_v + 1) = 45,150$. The other graphs in Figs. 16–18 are computed by the deterministic particle method. These graphs were previously shown in Figs. 9 and 10 for which the grid parameters are $N_x \times N_v = 100 \times 100 = 10,000$ particles, $\Delta t = 0.01$. The correspondence between the two methods seems quite good particularly in the graphs of ke and FE. As the steady state value of the kinetic energy is 2ke = 0.07 then as seen in Fig. 17 this limit is being approached somewhat more precisely by the deterministic particle computation. There is some discrepancy between the two methods in the graph of ese. The electrostatic energy is a relatively small quantity and is the most sensitive to changes in the computational method. The different ways of distributing the initial data points may account for the difference in the two ese graphs.

In drawing some comparison between the finite difference method and that of Section 2 it appears that the method of Section 2 has a higher order of accuracy. This can primarily be due to the fact that with the method of Section 2 the parameter Δt can be refined independently of Δx_0 and Δu to reduce the error. We conjecture based on the computations of Section 3.1 that the error for the method is of the form $O((\Delta x_0)^2 + (\Delta u)^2 + \Delta t)$. For the finite difference method the parameter Δt cannot be taken independently of Δx and Δv. A bound on the error for the time interval $[0,T]$ given in [14] is of the form

[1] The computer program for doing these calculations was provided to us by the author of [14].

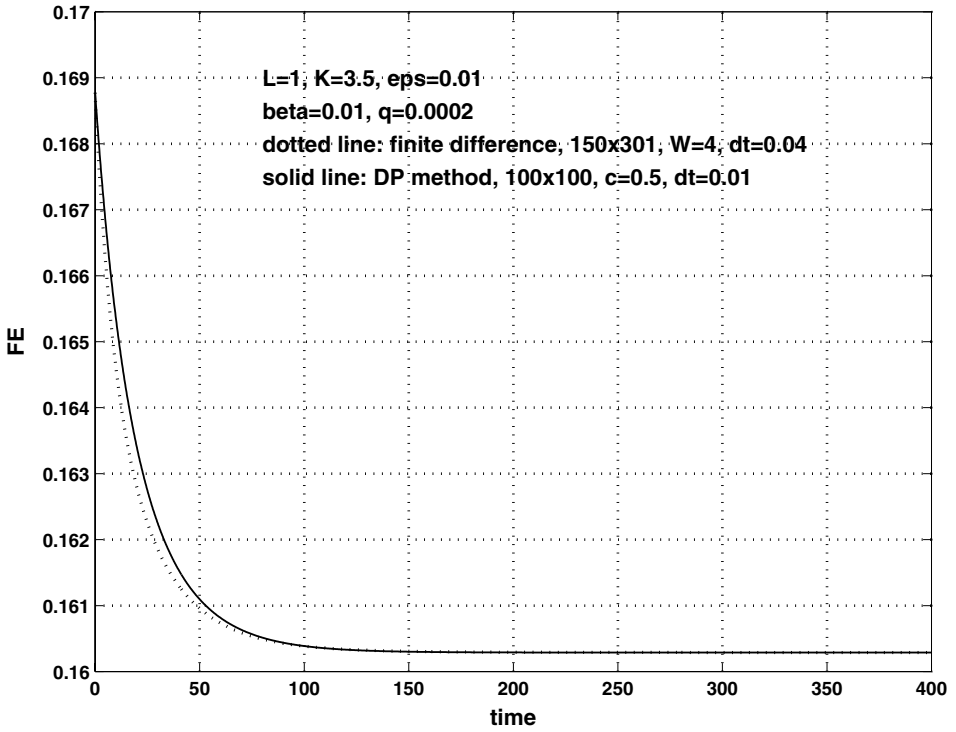

Fig. 18.

$$K(W)\left[\Delta t + \frac{(\Delta x)^2 + (\Delta v)^2}{\Delta t} + \frac{e^{-CW^2}}{\Delta t}\sqrt{1 + \frac{\Delta t}{\Delta v}}\right]. \tag{4.11}$$

Here W is the upper bound on velocity in region $\mathscr{A}$, $K(W)$, a certain function of W, and C a constant. According to this estimate for a given Δx, Δv, and W there is an optimal Δt that gives the minimal error. No claim is made in [14] that the bound (4.11) is optimal, and we do not attempt to verify the estimate computationally. However, our computations do indicate that an expression of the type (4.11) can be representative of the error for the finite difference method. For Δx, Δv, and W fixed as Δt is decreased the error will initially decrease to a certain point and then as Δt is further decreased the error of the method increases. It therefore becomes necessary to choose Δt close to the optimal value to minimize the error. Based on the estimate (4.11) and some experimentation we expect that Δt should be chosen such that $\Delta t = K\sqrt{(\Delta x)^2 + (\Delta v)^2}$, K a constant. However, there is uncertainty as to how to choose K, and changes in this parameter can have a notable effect on the computed solution.

To demonstrate the effect that varying Δt can have on the finite difference method we consider the free energy graphs of Fig. 18 and observe the approach to steady state on a fine scale. Fig. 19 gives the free energy graphs for the finite difference method with $W = 4$, $M_x, M_v = 150,150$ (45,150 data points) and $\Delta t = 0.05, 0.04, 0.03, 0.02$. As the steady state free energy is a lower bound for the free energy it is apparent that there is a loss of accuracy in the graphs for $\Delta t = 0.03, 0.02$. Here the graphs go below the steady state value with the loss of accuracy more pronounced in the graph for $\Delta t = 0.02$. The optimal Δt for this computation seems to be around $\Delta t = 0.04, 0.05$, and the graphs for these Δt values give a more accurate

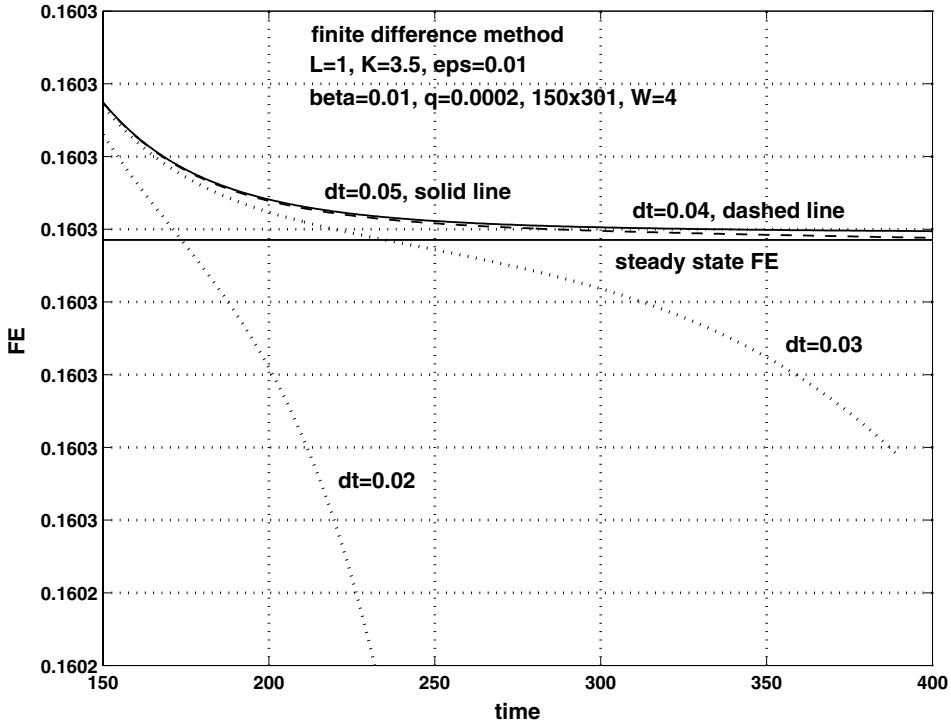

Fig. 19.

representation for the approach to the limit. Fig. 20 shows the approach to steady state given in Fig. 19 for which the scale is further refined. Included in Fig. 20 is the FE graph computed by the deterministic particle method for which $N_x \times N_v = 100 \times 100$, $\Delta t = 0.01$ (shown in Fig. 18). Also included for a point of reference is the FE graph computed with the deterministic particle (DP) method with $N_x \times N_v = 50 \times 50$, $\Delta t = 0.04$, $N_g = 100$. The jump discontinuities apparent in the DP graphs on this scale are due to the regriding. The regriding preserves kinetic energy but not entropy, so the ke graph is smooth but the entropy has discontinuities at the regriding points. For the solution computed by the DP method and $N_x \times N_v = 100 \times 100$ the convergence in the time parameter is largely complete with $\Delta t = 0.01$ and further reducing Δt makes an insignificant change in the solution. The exact steady state value of the free energy is FE = 0.16028852, and the solution computed with the deterministic particle method, $N_x \times N_v = 100 \times 100$, $\Delta t = 0.01$, is converging at $T = 400$ to the value FE = 0.16028863 (taken at the end of the particle cycle before regriding). This computation based on the deterministic particle method is giving a somewhat more precise answer for the limiting value of FE than is being obtained by the finite difference method.

To further study the convergence of the finite difference method we consider the solution obtained with $M_x \times (2M_v + 1) = 150 \times 301$ data points, $W = 4$, $\Delta t = 0.04$, refine the grid, and observe the effect on the graph of kinetic energy. Fig. 21 shows the approach to steady state in the graph of kinetic energy on a fine scale. The three graphs for the finite difference method are for grid parameters $W = 4$, $M_x \times (2M_v + 1) = 150 \times 301$, 200×401, 300×601, with $\Delta t = 0.04$, 0.03, 0.02, respectively. Thus in reducing Δx, Δv, and Δt the ratios $\Delta x/\Delta v$ and $\Delta x/\Delta t$ are constant. Also included in Fig. 21 are the *KE* graphs for the deterministic particle method with $c = 0.5$, $N_x \times N_v = 100 \times 100$, $\Delta t = 0.01$ and $c = 0.5$, $N_x \times N_v = 50 \times 50$, $\Delta t = 0.04$. It is evident that the computed solutions with the finite difference method approach more pre-

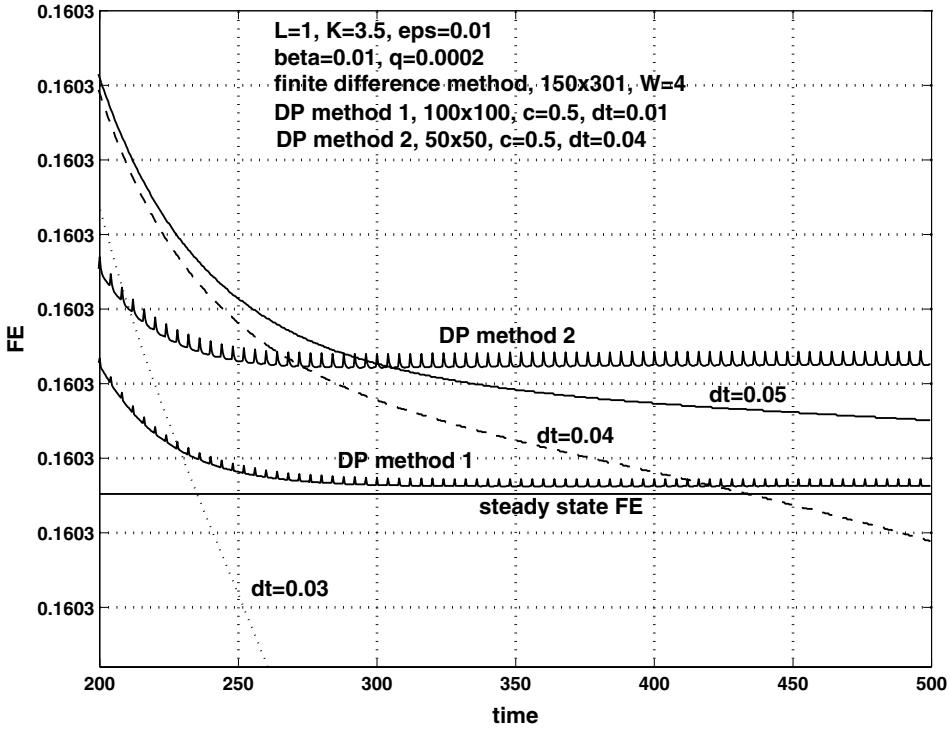

Fig. 20.

cisely the steady state value for the kinetic energy as the grid is refined. However, the approach to the steady state KE computed with the deterministic particle method is still more accurate and is obtained with significantly fewer data points.

Based on the present computations as well as others we have done we conclude that one can obtain good results with the finite difference method. It is, however, necessary to make a correct choice of Δt in order to get the best accuracy, and there is some uncertainty as to how to choose an optimal Δt. With the method of Section 2 there can be less uncertainty as to how to choose the parameters. For a given Δx_0 and Δu we decrease Δt until there is negligible change in the computed solution. Usually the regrid parameter, N_g, is set so that regriding is done at the same points in time for the different Δt. Refining Δt then gives the most accurate solution for a given Δx_0 and Δu. In addition, the computations indicate that the method of Section 2 has a higher order of accuracy than the finite difference method. The finite difference method is a simpler numerical procedure and for a given number of data points computationally significantly faster. However, as the method demonstrates lower accuracy one may obtain a comparably accurate solution with less computing resources using the method of Section 2. For example, we consider the solution to (1.1) and (1.2) of Figs. 16–18. The computation with the finite difference method uses $150 \times 301 = 45{,}150$ data points and $\Delta t = 0.04$. With the deterministic particle method a solution to this problem of comparable accuracy is computed with $50 \times 50 = 2500$ data points and $\Delta t = 0.04$, $N_g = 100$. The FE and ke graphs for this computation are shown on a fine scale in Figs. 20 and 21. With these parameters computed to $T = 500$ the DP method required about 0.54 times the computer memory and about 0.46 times the running time as the computation with the finite difference method. The computations were done on a Pentium based Linux workstation.

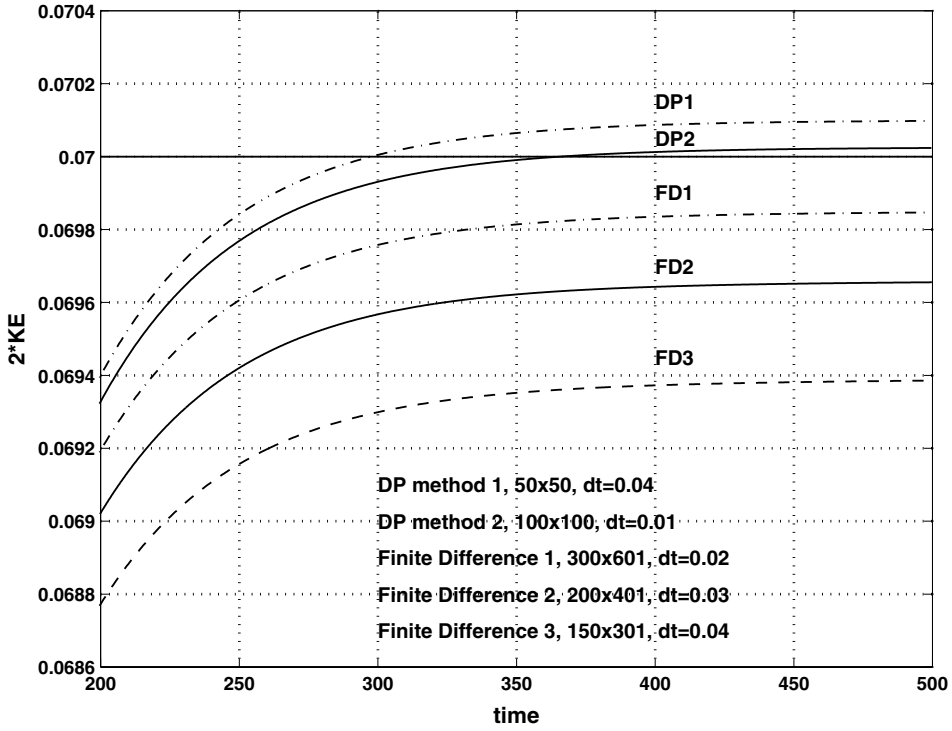

Fig. 21.

5. Conclusion

The numerical method presented is a deterministic type of particle method combined with a process for periodically reconstructing the distribution function on a fixed grid. The computations indicate that the numerical procedure is convergent and accurate over an extended time interval. By a transformation of variables based on characteristic equations associated with the transport part of (1.1), Eq. (1.1) is put into a form so that numerical methods for parabolic type partial differential equations can be applied. A direct method, Douglas–Rachford, and an iterative procedure, SOR, are outlined for solving the transformed Eq. (1.21) as a part of the particle method cycle of the computation. For small values of the diffusion parameter SOR is the more efficient method of approximation. This is because with small q in (1.1) the iterative procedure is rapidly convergent requiring relatively few iterations. Thus the PDE (1.21) is solved rather quickly at each step of the particle computation. The regriding of the approximate distribution function is introduced so as to limit the time interval on which the particle method is applied. This greatly enhances the long term stability of the numerical method. In comparison with some other methods of approximating (1.1) and (1.2) we find that the present method gives a higher degree of accuracy in the computed solution and with relatively fewer data points for the initial distribution function.

Acknowledgements

We would like to thank Professor Andrew Poje of the College of Staten Island for some very useful suggestions. We also want to thank Professor Jack Schaeffer of Carnegie Mellon University for the use of a

computer program that implements the numerical method of [14], and we want to thank the referees for helpful comments and suggestions.

References

[1] E.J. Allen, H.D. Victory Jr., A computational investigation of the random particle method for numerical solution of the kinetic Vlasov–Poisson–Fokker–Planck equations, Phys. A 209 (1994) 318–346.
[2] W.F. Ames, Numerical Methods for Partial Differential Equations, Barnes and Noble, Inc, New York, 1971.
[3] F. Bouchut, J. Dolbeault, On long time asymptotics of the Vlasov–Fokker–Planck equation and of the Vlasov–Poisson–Fokker–Planck system with coulombic and Newtonian potentials, Diff. Integral Eq. 8 (3) (1995) 487–514.
[4] J.P. Boyd, Chebyshev and Fourier Spectral Methods, Lecture Notes in Engineering, vol. 49, Springer-Verlag, Berlin, 1989.
[5] S. Chandrasekhar, Stochastic problems in physics and astronomy, Rev. Mod. Phys. 15 (1943) 1–89.
[6] C.-C. Chang, Random vortex methods for the Navier–Stokes equation, J. Computat. Phys. 76 (1988) 281–300.
[7] C. Cheng, G. Knorr, The integration of the Vlasov equation in configuration space, J. Computat. Phys. 22 (1976) 330–351.
[8] R. Courant, Differential and Integral Calculus, vol. II, Interscience Publishers Inc, New York, 1968.
[9] K.J. Havlak, H.D. Victory Jr., The numerical analysis of random particle methods applied to Vlasov–Poisson–Fokker–Planck kinetic equations, SIAM J. Numer. Anal. 33 (1996) 291–317.
[10] K.J. Havlak, H.D. Victory Jr., On deterministic particle methods for solving Vlasov-Poisson–Fokker–Planck systems, SIAM J. Numer. Anal. 35 (4) (1998) 1473–1519.
[11] P.E. Kloeden, E. Platen, Numerical Solution of Stochastic Differential Equations, Springer -Verlag, New York, 1992.
[12] H. Neunzert, J. Wick, The convergence of simulation methods in plasma physics, in: R. Kress, J. Wick (Eds.), Mathematical Methods of Plasma Physics, 1980.
[13] C.E. Rathmann, J. Denavit, Simulation of collisional effects in plasmas, J. Computat. Phys. 18 (1975) 165–187.
[14] J. Schaeffer, Convergence of a difference scheme for the Vlasov–Poisson–Fokker–Planck system in one dimension, SIAM J. Numer. Anal. 35 (3) (1998) 1149–1175.
[15] J. Schaeffer, A difference scheme for the Vlasov–Poisson–Fokker–Planck system, Research Report No. 97-NA-004, Department of Mathematical Sciences, Carnegie Mellon University, 1997.
[16] J.W. Thomas, Numerical Partial Differential Equations, Springer-Verlag, New York, 1995.
[17] H.D. Victory Jr., B.P. O'Dwyer, On classical solutions of the Vlasov–Poisson–Fokker–Planck systems, Indiana Univ. Math. J. 39 (1990) 105–156.
[18] S. Wollman, E. Ozizmir, R. Narasimhan, The convergence of the particle method for the Vlasov–Poisson system with equally spaced initial data points, Transport Theory Statist. Phys. 30 (1) (2001) 1–62.
[19] S. Wollman, E. Ozizmir, Numerical approximation of the one-dimensional Vlasov–Poisson system with periodic boundary conditions, SIAM J. Numer. Anal. 33 (4) (1996) 1377–1409.
[20] S. Wollman, E. Ozizmir, A numerical method for the Vlasov–Poisson–Fokker–Planck system in one dimension. In: Proceedings of Neural, Parallel, and Scientific Computations, vol. 2, 2002, pp. 179–182.